ZMYND11 REGULATES BLOOD CELL DEVELOPMENT IN ZEBRAFISH

by

AIMEE KOWALSKI

(Under the Direction of Scott Dougan)

ABSTRACT

For an embryo to develop properly from a single cell into a complex multicellular organism with several cell types having specialized functions requires rapid morphological changes throughout the entire embryo that must be tightly regulated. Underlying the development of each cell type, is an intricate coordination of gene expression specific to that cell type which changes as the cell matures and differentiates. The chromatin state of a gene has increasingly been found to be important for proper gene expression, with open euchromatin being accessible to proteins that modulate transcription, and heterochromatin silencing transcription. The state of chromatin is controlled by several chromatin writer and eraser proteins that post-translationally modify histone tails to confer a more open or closed chromatin confirmation and recruit chromatin readers to influence target gene transcription. One such reader protein, *ZMYND11*, has been shown to specifically bind histone variant H3.3, which is incorporated into transcriptionally active genes. Once bound to chromatin, *ZMYND11* recruits other proteins to modulate target gene expression, although the mechanism underlying *ZMYND11*'s ability to regulate gene expression is poorly understood.

Interestingly, *ZMYND11* has been found to be mutated in blood cancers and patients born with *ZMYND11* haploinsufficiency experience recurrent infections. To better understand the

function of *zmynd11* in blood cell development, we created a mutant line of zebrafish. Our studies show that in the absence of *zmynd11*, primitive red blood cells over-proliferate and may have problems properly specifying cell fate. Specifically, RNA-seq analysis found that several genes involved in proliferation and master regulators of erythrocyte lineage specification were dysregulated, as well as the upregulation of several heat shock proteins that are primarily expressed in response to cellular stress. Our results show that *zmynd11* is required for proper proliferation and lineage specification of primitive erythrocytes in zebrafish.

INDEX WORDS: ZMYND11, Histone H3.3, chromatin, nucleosome, erythrocyte

ZMYND11 REGULATES BLOOD CELL DEVELOPMENT IN ZEBRAFISH

by

AIMEE KOWALSKI

B.S., The University of Alabama at Birmingham, 2007

M.S., Georgia State University, 2012

A Dissertation Submitted to the Graduate Faculty of The University of Georgia in Partial Fulfillment of the Requirements for the Degree

DOCTOR OF PHILOSOPHY

ATHENS, GEORGIA

2025

ZMYND11 REGULATES BLOOD CELL DEVELOPMENT IN ZEBRAFISH

by

AIMEE KOWALSKI

Major Professor: Scott Dougan

Committee: Edward Kipreos
Jonathan Eggenschwiler
Amy Medlock

Electronic Version Approved:

Ron Walcott
Vice Provost for Graduate Education and Dean of the Graduate School
The University of Georgia
December 2025

DEDICATION

We are all a product of our genetics and environmental influences – I learned this in biology class and can clearly see it in my own life. I would not be where I am now without my family, and each person has contributed to the person I am now. My maternal grandmother, emphasized the importance of education so I always took school seriously; my paternal grandfather gave me the gift of a mathematical, problem-solving mind, which is definitely an asset in science and research; my paternal grandmother made me a perfectionist, which ensures my confidence in my research knowing that I pay close attention to every detail; and my maternal grandfather gave me the gift of gambling, because I never wouldn't have taken the chance to move away for graduate school without a propensity for taking risks.

My mom and dad were always my biggest supporters and encouraged me to pursue any career I wanted. My mother also valued education and taught me that it was never too late to go back to school when she was accepted to nursing school at the age of 43. My dad, much like his dad, instilled in me a mechanical mind and the grit to set goals and accomplish them through hard work and dedication.

No one knows you like your sibling. My sister, Natalie, organized most of my wedding since I was in my first year of graduate school and didn't have the time, then she searched all of Athens for preemie clothes when Bonnie was born five weeks early. She always showed up when I needed her, and graduate school would have definitely been harder without her.

Finally, my husband, Chris, and daughter, Bonnie, have been supportive beyond belief! Chris relocated for me to go to graduate school, even though it took us farther away from family.

It was difficult having a child and not being close to family, but he helped every way he could when it came to parenting. The countless number of times he had to pick up Bonnie from school with only a few minutes notice because I needed a few more minutes to finish up my experiments that day and things like the hours spent taking her to the playground or anywhere else but our home while I wrote my qualifying exams. I could not have completed my dissertation without him! I truly could not have asked for a better daughter than Bonnie! She has been so understanding, especially this past year. I worked late a lot, and we ate out a lot, but she never complained even though I could tell that she was getting a little tired of Papa John's. When I asked for help taking care of things around the house because I was so busy, she did it without question. She could see the stress I was under, and she stepped up! My nephew Julian has also been extremely understanding of the stress of this year especially. I've forgotten so many things, had to delay trips to visit family, and he also had his fill of Papa John's (we all did) but he's hasn't complained.

For *all* these reasons, I dedicate this dissertation to *all* of these people because they all helped make it happen.

ACKNOWLEDGEMENTS

Special thanks to Dr. Juan Bustamante for all his help with flow cytometry and answering all my questions about how the machines work and how to sort my cells and analyze the results. A huge thank you to Dr. Canaan Whitfield-Cargile for all the help processing and analyzing the RNA-seq data, without which I would have been completely lost. Dr. Megan Meany helped tremendously with deciding on which reagents I needed for RNA isolation and library prep for RNA-seq.

I also want to acknowledge all the hard work done by my two undergraduates, Sarah Gayle Hammond and Magdalene Ellis. Sarah Gayle was so helpful in the early stages of this project and really helped grind out the genotyping to establish mutant lines. Magdalene did a lot of work on the craniofacial defects of mutant zebrafish to find the best way to get images of Meckel's cartilage with single cell resolution.

Huge thanks to all my lab mates, past and present, Wei-Chia Tseng, Munisa Mumingjiang, Suganthan Amirthagunanathan, and Nurgul Kaya. I'm so glad that I was able to turn to them with my lab problems, from switching fish feeding days to talking through failed experiments.

Thank you to my PI and committee members, Dr. Scott Dougan, Dr. Edward Kipreos, and Dr. Amy Medlock, and Dr. Jonathan Eggenschwiler, for their continued patience and guidance during graduate school. Dr. Dougan allowed me to follow the project I wanted and trusted me to make critical decisions in the direction of my project. Dr. Medlock, in particular, helped so much with fish room maintenance and gave me the *lcr:GFP* zebrafish which were

instrumental to my dissertation studies. Dr. Kipreos was always interested in helping me with my project, asking me about my progress almost every time I saw him and suggesting ways to help with problems. Additionally, Dr. Jim Lauderdale was always supportive throughout my time at UGA, as a PI and as Department Head. I'm grateful that he made his equipment accessible for students outside his lab, including both fluorescent microscopes, which I used regularly.

Joelle Szendel, Dr. Nancy Manley, Dr. Jonathan Eggenschwiler, Dr. Doug Menke, and Dr. Nancy Manley have done so much work organizing the DevBio Alliance events and DevBio RIP. I look forward to the retreat and symposium every year and the RIP meetings keep me connected with people in the DevBio community at UGA.

TABLE OF CONTENTS

Page

LIST OF FIGURES

Page

LIST OF TABLES

Page

CHAPTER 1

INTRODUCTION AND LITERATURE REVIEW

The role of chromatin in regulation of gene expression

The developing embryo undergoes constant morphological change as it grows from a single cell into a multicellular organism with several different organs of specialized function. The cascade of spatiotemporal gene expression required to precisely generate numerous cell types in an organism requires perfectly timed gene regulation, so that the genes required for maintenance and proliferation of stem cells are turned off and genes that define a mature cell's identity and function are turned. Several mechanisms exist to regulate gene expression, including the DNA sequence, DNA methylation, transcription factors, RNA processing, and the chromatin state of target genes.

Chromatin is composed of nucleosomes, which are made of approximately 146bp DNA wrapped around a protein complex, which is composed of a highly conserved octamer of histones H2A, H2B, H3, and H4. Each histone protein consists of a globular domain that interacts with other histones in the nucleosome core which is wrapped ~1.7 times by DNA, as well as an N-terminal tail that hangs out of the nucleosome. (Luger, 1997) Normally, histones are expressed in high amounts during S phase of the cell cycle, since twice as much DNA requires twice as many histones to compact the DNA into chromosomes. Histones that exhibit high expression during S phase are known as canonical histones and they are incorporated into chromatin in a DNA synthesis-coupled manner. Additionally, histone variants with specialized functions, known as replacement histones, can be incorporated into nucleosomes to provide

regulation of target gene expression. In contrast to canonical histones, these distinct replacement histone variants are not highly expressed during S phase and are incorporated into chromatin independent of DNA synthesis. (Ahmad & Henikoff, 2002; Brown et al., 1985; Wu et al., 1982; Wunsch & Lough, 1987)

In recent years, several variants of all histones have been discovered, with some variants showing lineage specific expression and some expressed universally. The most relevant for the purposes of this review is Histone H3, for which a total of eight variants have been discovered so far. In mammals, histones H3.1 and H3.2 are considered canonical H3 histones, whereas H3.3, H3t, H3.X, H3.Y, H3.5 and CENP-A are replacement histones (Albig et al., 1996; Palmer et al., 1987; Schenk et al., 2011; Sullivan et al., 1994; Witt et al., 1996). Specifically, histone H3.3 differs from the canonical H3.1 and H3.2 by only five and four amino acid residues, respectively, and the peptide sequence of H3.3 is remarkably 100% conserved across all higher order eukaryotes. However, despite the similarity in protein sequence, the chromosomal arrangement and mRNA processing of canonical histones H3.1 and H3.2 differs greatly are from that of H3.3. Whereas H3.1 and H3.2 are arranged in clusters of multiple gene copies and do not have introns or polyadenylated tails, H3.3 does contain introns and a polyadenylated tail and has only a single or very few copies distributed throughout the genome, depending on the organism. (Engel et al., 1982; Franklin & Zweidler, 1977)

Only one residue, serine 31, differs between the tails of H3.3 and canonical histones H3.1 and H3.2. In canonical histones, residue 31 is alanine, which cannot be modified, whereas serine can be post-translationally modified, including phosphorylation and acetylation. The other 3 to 4 amino acids that differ between H3.2 and H3.1 versus H3.3, respectively, are in the globular core and are essential for proper nucleosome assembly. Residues 87, 89, and 90 are different between

H3.3 and the canonical H3 variants, with H3.1 also differing at residue 96. Mutation studies have shown that changing these amino acids to make one variant more like the other variant changes its deposition onto chromatin. (Ahmad & Henikoff, 2002; Goldberg et al., 2010) Additionally, in contrast to canonical histones H3.1 and H3.2, Histone H3.3 is incorporated into chromatin in a replication-independent manner, with two different protein complexes regulating its incorporation, depending on location in the genome. The HIRA complex incorporates H3.3 into euchromatin, including promoter regions, gene bodies of actively transcribed genes, and regulatory elements (Chow et al., 2005; Ray-Gallet et al., 2010; Ricketts et al., 2015; Tagami et al., 2004; Wirbelauer et al., 2005), whereas DAXX and ATRX incorporate H3.3 into areas of heterochromatin such as telomeres and pericentric DNA repeats (Drane et al., 2010; Elsässer et al., 2012; Lewis et al., 2010; Liu et al., 2012). Interestingly, transcription from heterochromatic pericentric repeats has been reported (Lu & Gilbert, 2007), and expression is decreased when DAXX is mutated or when H3.3 or ATRX is knocked down, suggesting that H3.3 deposition is required for proper transcriptional activation from these regions (Drane et al., 2010).

In addition to controlled incorporation of histone variants, the N-terminus end of each histone that hangs out of the nucleosome can be chemically modified by methylation, acetylation, or phosphorylation on lysine, arginine, serine, threonine, and tyrosine residues to regulate gene expression and control chromatin compaction. For the purposes of this review, we will focus on lysine methylation, which can be a mark of active or repressive transcription. In general, methylation of lysines 4, 36, and 79 on H3 (H3K4, H3K36 and H3K79) normally marks transcriptional activation, while methylation on lysines 9 and 27 of H3 and lysine 20 on H4 (H3K9, H3K27 and H4K20) are associated with transcriptional inhibition. Furthermore, each

lysine can be monomethylated (me1), dimethylated (me2), or trimethylated (me3), adding to the regulatory complexity of gene expression control. (Millán-Zambrano et al., 2022)

The state of post-translational modifications influences how open the chromatin is and how accessible the target gene DNA is by changing the charge of the histone tails. Additionally, the combination of histone variant plus chemically modifying (i.e. acetylation, methylation, etc.) specific histone residues of a target gene may act as a code for determining the amount of gene expression and potentially the isoform of the gene product. This "histone code", which is regulated by an intricate system of chromatin writers and erasers, presumably determines the transcriptional activity of target genes through its specific recruitment of proteins called chromatin readers, which recognize the specific histone modification and assemble other proteins to mediate gene expression. Chromatin writers are proteins that catalyze the post-translational addition of chemical groups to specific histone residues, and, in the case of methylation, they are called histone methyltransferases (HMT), while chromatin erasers remove chemical modifications on histones and are known as histone demethylases (HDM) if it catalyzes the removal of methyl groups from histone residues. Furthermore, writers and erasers can only catalyze the addition or removal of certain post-translational modifications (PTM) on specific histone residues and in some cases, are expressed in a tissue-specific manner. For example, Lysine-Specific Methyltransferase 2A (KMT2A) is only able to methylate lysine 4 on H3 and its expression has been shown to be important in developing hematopoietic and neural tissues, since KMT2A loss of function mutations have been associated with both leukemia and intellectual disability (Chan et al., 2019; Yang & Ernst, 2017).

ZMYND11 is a Histone H3.3 variant-specific chromatin reader

ZMYND11 (zinc finger MYND-type containing 11, formerly known as BS69) was originally identified because it suppressed transcriptional activity of the adenoviral E1A oncoprotein and was later shown to inhibit activity of the transcription factor c-Myb in yeast transactivation assays (Hateboer et al., 1995; Ladendorff et al., 2001). The ZMYND11 protein contains a MYND domain on the C-terminus, which mediates its interaction with proteins known to be involved in gene regulation, including transcription factors, RNA splicing related proteins, and chromatin remodeling proteins (Figure 1.1) (Ekblad et al., 2005; Ladendorff et al., 2001; Masselink & Bernards, 2000; Velasco et al., 2006). Additionally, the N-terminus is comprised of three tandemly arranged, putative chromatin binding domains, namely a plant homeodomain (PHD), a bromodomain (BROMO), and a PWWP domain. It is through the BROMO-PWWP motif that ZMYND11 specifically recognizes lysine 36 trimethylation on histone variant H3.3 (H3.3K36me3), making ZMYND11 the first histone variant-specific chromatin reader protein to be identified. Additionally, crystallography studies showed ZMYND11 interacts with amino acids alanine 29 to histidine 39 of H3.3, which explains its specificity for H3.3 since serine 31 is one of the few amino acid differences between H3.3 and canonical histones H3.1 and H3.2 (Wen et al., 2014).

Interestingly, phosphorylated serine 31 on Histone H3.3 (H3.3S31) abolishes ZMYND11 binding and therefore could be used to control ZMYND11's ability to bind to chromatin and regulate target gene expression (Guo et al., 2014). Furthermore, H3.3S31 phosphorylation was shown to increase acetylation of neighboring nucleosomes, leading to an increase in target gene transcription (Martire et al., 2019). Since ZMYND11 interacts with histone deacetylases (HDAC), H3.3S31 dephosphorylation could be used as a switch to repress gene expression.

Furthermore, ChIP-seq analysis revealed a genome-wide co-localization of ZMYND11 with H3K36me3 and H3.3 in gene bodies, and its occupancy requires the pre-deposition of H3.3K36me3 (Guo et al., 2014; Wen et al., 2014). At first, this may seem counterintuitive given the association of H3.3K36me3 with actively expressed genes (Goldberg et al., 2010; Mito et al., 2005; Tagami et al., 2004; Venkatesh et al., 2012). However, taken together it provides a model whereby H3.3K36me3 is likely laid down as active genes are transcribed which eventually recruits ZMYND11 to repress gene expression, though the molecular mechanisms underlying ZMYND11's ability to mediate transcription are not completely understood.

Recent publications have reported evidence for differing although not mutually exclusive, mechanisms of ZMYND11 repression. Guo et al. showed that ZMYND11 promotes intron retention, which leads to degradation of mRNA, reducing target gene transcript levels as a result. This model is supported by evidence that ZMYND11 antagonizes core RNA splicing machinery through its direct interaction with EFTUD2, which was also shown to be dependent on ZMYND11's association with H3.3K36me3 (Guo et al., 2014). Alternatively, Wen et al. showed that ZMYND11 may repress gene expression by preventing paused RNA polymerase II from releasing and entering elongation. They hypothesize that ZMYND11 is regulating the local chromatin environment through its interaction(s) with members of the SWI/SNF chromatin remodeling complex, thereby preventing RNA Polymerase II from entering gene bodies (Wen et al., 2014). Currently, it is not clear if this aspect of ZMYND11 function also requires interaction with H3.3K36me3 or whether some other mechanism is responsible. However, considering that ZMYND11 directly interacts with several transcription factors (Ansieau & Leutz, 2002; Ekblad et al., 2005; Ladendorff et al., 2001; Velasco et al., 2006; Wei et al., 2003), which can function to either directly or indirectly mediate RNA Pol II activity, it is feasible that they could be

regulating this aspect of ZMYND11's function.

Possible unexplored mechanism of *ZMYND11* target gene regulation

We propose an additional mechanism where *ZMYND11* also contributes to *de novo* repression of genes needed to maintain the proliferative capacity of stem cell populations, as is the case with Polycomb-mediated gene silencing in lineage specification. In a well-established example, Polycomblike (PCL) binds H3K36me3 to facilitate recruitment of Polycomb group (PcG) proteins, which remodels the local chromatin environment to repress transcription of previously active embryonic stem cell-specific genes, thus allowing for proper differentiation (Abed & Jones, 2012; Ballaré et al., 2012; Brien et al., 2012; Musselman et al., 2012). ZMYND11's specific recognition of H3.3K36me3 together with its interaction with several chromatin-remodeling proteins, suggest a mechanism where ZMYND11 could contribute to lineage specification by similarly suppressing transcription of genes required to maintain pluripotency.

In fact, ZMYND11 interacts with CBX4, PH3, and BCORL1, which are part of PRC1, as well as EZH2 which is a catalytic component of PRC2 that methylates H3K27. Furthermore, ZMYND11 has been shown to interact with several members of the noncanonical polycomb repressive complex 1.6 (PRC1.6), which include MGA, E2F6, L3MBTL2, RING1/2, and HDAC. Additionally, L3MBTL2 recognizes methylation on H3K4, H3K9, H3K27, and H4K20 and another member of PRC1.6, HP1gamma, recognizes di- and tri-methylation on H3K9. Moreover, ZMYND11 interacts with chromatin writers and erasers, including KMT2A, NSD1, and KDM3B, that control lysine methylation at H3K4, H3K9, H3K36, although it's not known if ZMYND11 enhances or inhibits their ability to modify histone tails. However, it's possible that ZMYND11 not only directly recruits PRC1.6 to target genes through protein-protein interactions

but also regulates the surrounding histone tail modifications to encourage PRC1.6 recruitment through its recognition of specific lysine methylation states. Furthermore, ZMYND11 could recruit chromatin remodelers to open up the regions containing MGA and E2F6 DNA binding sequences.

Stielow et. al. (2018) proposed a mechanism whereby PRC1.6 is recruited to target genes primarily through the transcription factors MGA and E2F6 recognizing their respective DNA binding domains. However, little credit is given to the chromatin state of target genes or other proteins that could be recruiting PRC1.6. Given that ZMYND11 interacts with several members of the PRC1.6, I believe that ZMYND11 is recruiting PRC1.6 to a subset of MGA/E2F6 target genes to modulate expression.

ZMYND11 is Required for neural, craniofacial, and blood development

During neurogenesis, an extensive battery of genes encoding components of the synaptic transmission machinery and specialized cytoskeletal proteins are activated, though the mechanisms regulating these genes are not well understood. Several human case studies have demonstrated a causal link between *ZMYND11* loss of function mutations and intellectual disability, autism and schizophrenia. Interestingly, these patients also had characteristic craniofacial features, such as a wide or depressed nasal bridge and low-set eyes, showing that *ZMYND11* is clearly involved in neural and craniofacial development (Cobben et al., 2014; Coe et al., 2014; DeScipio et al., 2012; Tumiene et al., 2017; Vargiami et al., 2014; Yates et al., 2020a). Additionally, whole exome sequencing of patients previously diagnosed with dystonia, a neurological disorder that results in muscle contraction and twitching, identified two patients with mutations in *ZMYND11* (Thomsen et al., 2025). Yu et al. (2009) showed that *ZMYND11* is normally downregulated in neurons as they differentiate, however, if *ZMYND11* expression

levels are maintained by transfection, lineage specification is inhibited, suggesting that ZMYND11 could be repressing lineage-specific gene expression and its downregulation is required for cells to completely differentiate.

In addition to the neural and craniofacial phenotypes seen in patients with *ZMYND11* haploinsufficiency, several of them experience recurrent infections, indicating a problem with immune system function, which could include aberrant development of immune cells (Bodetko et al.; Tumiene et al., 2017). Furthermore, several types of leukemia have been identified with *ZMYND11* loss of function mutations. Copy number variations, meaning deletions or duplications of pieces of genomic DNA that can be hundreds to several kilobases long, that include *ZMYND11* have been found in several types of leukemias and myelomas (Yang et al., 2010). Additionally, numerous cases of acute myeloid leukemia (AML) have been reported with recurrent translocations, t(10; 17) (p15; q21), which produce a ZMYND11-MBTD1 fusion protein that contains only the N-terminal chromatin binding domain of ZMYND11 fused with either full length or all but the first 2 exons of Malignant Brain Tumor Domain Containing 1 (MBTD1) (Braekeleer et al., 2014; Kawai et al., 2024; Plesa & Sujobert, 2019; Rooij et al., 2015; Tempescul et al., 2007; Yamamoto et al., 2018). Because ZMYND11's chromatin binding domain is preserved, ZMYND11-MBTD1 still recognizes H3.3K36me3, but with no MYND domain to recruit the usual partners to mediate gene expression, the MBTD1 portion recruits the histone acetyltransferase complex NuA4/TIP60, which increases target gene expression. As a result, AML arising from this translocation is poorly differentiated and the characteristic set of upregulated genes increases the "stemness" potential of these cancerous blood cells. (Devoucoux et al., 2022; Li et al., 2021).

In regards to ZMYND11's interaction with PRC1.6, it is worth noting that losing function of any one of the members of PRC1.6, Histone H3.3, or K36me3 independently have been implicated as causal mutations leading to leukemia (Attieh et al., 2013; Paoli et al., 2013; Tanaskovic et al., 2022). Additionally, the chromatin writers that ZMYND11 is known to interact with, NSD1, KDM3B, and KMT2A, have been found to be mutated in leukemias (Guarnera et al., 2024; Kim et al., 2023; Yang et al., 2021; Yoo et al., 2024; Zehtabcheh et al., 2025). This highlights the importance of the cascade from H3.3 deposition, to lysine 36 trimethylation, followed by recruitment of ZMYND11, and presumably PRC1.6, in the development and lineage specification of blood cells.

Taken together, it seems that ZMYND11 plays a role in differentiation of many cell types, including neural, craniofacial, and blood cells, and this role is largely dependent on its interaction with H3.3K36me3. It's interesting that one protein could regulate lineage specification of such different tissue types, which require distinctive genes be turned on to confer each tissue's function. If ZMYND11 is in some ways a central protein in the universal gene regulatory machinery during cell differentiation, then the spatiotemporal tissue-specific expression of proteins important for ZMYND11's function are key to tissue-specific gene regulation. For example, the mechanisms that target H3.3 deposition and histone post-translational modifications and proteins that interact with ZMYND11 must be precisely regulated to modulate tissue-specific gene expression of downstream targets.

Zebrafish as a model organism to study blood development

Blood development in all vertebrates proceeds in two successive waves, first the primitive wave then the definitive wave. In mammals, the primitive wave begins to differentiate early on from mesoderm at the onset of gastrulation, and the first blood cells arise in the blood

islands of the yolk sac by E7.0 in mice. By E7.5, a semi-synchronous population of immature blood cells can be seen in mouse embryos which then undergo a limited number of cell divisions until E12.5. As the primitive erythroblasts mature, they undergo a series of morphological changes, including cytoskeletal remodeling, leading to a reduction in cell size and shrinking of the nucleus. By E16.5-17.5 the primitive wave of erythrocytes have lost their nuclei and matured to become reticulocytes, which is evident by a drastic decrease in surface area and volume (Fraser et al., 2006; Kingsley et al., 2004; McGrath et al., 2008). While the lifespan of a primitive red blood cell is not known, they have been found in circulation up to seven days after birth in mice. Although primitive wave research is limited in humans because of ethical concerns, the blood islands emerge by 18-20 days gestation, primitive erythrocytes are in circulation beginning at three to six weeks, and have been detected throughout the third trimester. By about the sixth week of development, the definitive wave appears in the human fetal liver and by about 32 weeks, the bone marrow has become the primary site for hematopoiesis (Chasis & Mohandas, 2008).

Both the primitive and definitive erythrocytes go through three stages of maturation. They begin developing in a protected space outside of the vascular system as progenitors, then become erythroblast precursors, and for the final stage, mature red blood cells enter circulation. Some of the same genetic pathways and transcriptional regulators are used in the development of both primitive and definitive waves, such as *GATA1, KLF1, TAL1, LMO2,* and *LDB1* (Hodge et al., 2005; Pevny et al., 1995; Robb et al., 1995). However, there are also differences between the two waves, most notable is the hemoglobin that is expressed in primitive compared to definitive waves. For example, even though both waves initially express embryonic zeta globin and switch to expressing the adult alpha globin, the definitive wave expresses much lower levels of zeta

globin, also expresses fetal gamma globin and switches to adult alpha globin earlier in maturation than the primitive wave. Additionally, expression of some key regulators of transcription, like *MYB, SOX6,* and *BCL11A* are only present in the definitive wave (Tober et al., 2008; Xu et al., 2010; Yi et al., 2006).

The primitive and definitive waves of blood development in zebrafish are analogous to humans, in that several of the same genes are required for proper lineage specification. However, the origin is slightly different in that it originates from the posterior lateral mesoderm at about 10-12 hours post fertilization, right at the end of gastrulation. These cells then migrate to the blood islands located at the anterior lateral mesoderm, where primitive monocytes are made, and the intermediate cellular mass, which generates primitive erythrocytes before 24hpf. The definitive hematopoietic stem cells bud from hemogenic endothelium on the ventral wall of the dorsal aorta and at about 3dpf a small subset of these cells migrate to the thymus to produce T lymphocytes and to the caudal hematopoietic tissue where several lineages of blood cells are produced. Finally, by 5dpf the hematopoietic stem cells seed the kidney, which is the final site of definitive hematopoiesis.

Approximately 70% of human proteins have a zebrafish homolog, underscoring the usefulness of model organisms in helping understand cellular processes and disease states that are common to both humans and zebrafish. Zebrafish use several of the same key regulators for lineage specification of erythrocytes and other blood cell types, including *gata1, tal1, klf1* and *lmo2* and the red blood cells undergo similar morphological changes and modifications to the cytoskeleton during differentiation. As red blood cells mature in zebrafish, they also become smaller with a smaller nucleus and less granular cytoplasm.

External fertilization, high fecundity, and transparent embryos make zebrafish the perfect model organism for studying developmental processes. Additionally, transgenic modifications in zebrafish have allowed cell type-specific expression of fluorescent reporter proteins to allow visualization of the cells of interest, which can be tracked in live embryos over time without the need to fix and stain samples. Combined with the ease of creating mutations in a particular gene of interest by injecting CRISPR Cas9 and guide RNAs into embryos at 1-cell stage allows for reverse genetics studies to understand the function of certain genes of interest.

Figures

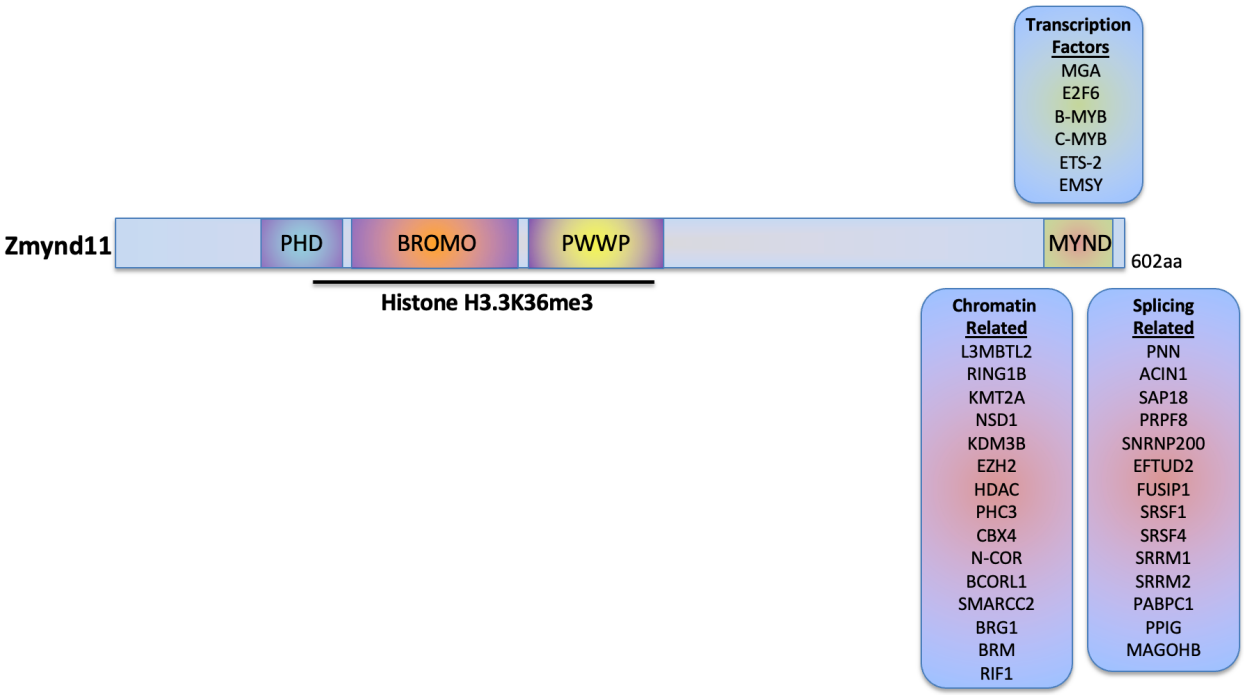

Figure 1.1. ZMYND11 interacting proteins. ZMYND11 interacts with trimethylated lysine on Histone H3.3 (H3.3K36me3) through its tandem PHD-BROMO-PWWP domain, while interacting with transcription factors, chromatin-related proteins, and splicing-related proteins.

References

Abed, J. A., & Jones, R. S. (2012). H3K36me3 key to Polycomb-mediated gene silencing in lineage specification. *Nat Struct Mol Biol*, *19*(12), 1214-1215.

Ahmad, K., & Henikoff, S. (2002). The Histone Variant H3.3 Marks Active Chromatin by Replication-Independent Nucleosome Assembly. *Molecular Cell*, *9*, 1191-1200. https://doi.org/https://doi.org/10.1016/S1097-2765(02)00542-7

Albig, W., Ebentheuer, J., Klobeck, G., Kunz, J., & Doenecke, D. (1996). A solitary human H3 histone gene on chromosome 1. *Human Genetics*, *97*, 486-491.

Ansieau, S., & Leutz, A. (2002). The Conserved Mynd Domain of BS69 Binds Cellular and Oncoviral Proteins through a Common PXLXP Motif. *Journal of Biolgical Chemistry*, *277*(7), 4906-4910.

Attieh, Y., Geng, Q.-R., DiNardo, C. D., Zheng, H., Jia, Y., Fang, Z.-H., Gañán-Gómez, I., Yang, H., Wei, Y., Kantarjian, H., & Garcia-Manero, G. (2013). Low frequency of H3.3 mutations and upregulated DAXX expression in MDS. *Blood*, *121*(19), 4009-4011. https://doi.org/https://doi.org/10.1182/blood-2012-11-466714

Ballaré, C., Lange, M., Lapinaite, A., Martin, G. M., Morey, L., Pascual, G., Liefke, R., Simon, B., Shi, Y., Gozani, O., Carlomagno, T., Benitah, S. A., & Croce, L. D. (2012). Phf19 links methylated Lys36 of histone H3 to regulation of Polycomb activity. *Nat Struct Mol Biol*, *19*(12), 1257-1265.

Beer, D. G., Kardia, S. L. R., Huang, C.-C., Giordano, T. J., Levin, A. M., Misek, D. E., Lin, L., Chen, G., Gharib, T. G., Thomas, D. G., Lizyness, M. L., Kuick, R., Hayasaka, S., Taylor, J. M. G., Iannettoni, M. D., Orringer, M. B., & Hanash, S. (2002). Gene-expression profiles predict survival of patients with lung adenocarcinoma. *Nature Medicine*, *8*(8), 816-824. https://doi.org/10.1038/nm733

Bodetko, A., Karpinski, P., Bladowska, J., Chrzanowska, J., Rydzanicz, M., Borys-Iwanicka, A., Ploski, R., & Smigiel, R. Further Delineation of Clinical Phenotype of ZMYND11 Variants in Patients with Neurodevelopmental Dysmorphic Syndrome. *Genes*, *15*(256). https://doi.org/doi.org/10.3390/genes15020256

Braekeleer, E. D., Auffret, R., Douet-Guilbert, N., Basinko, A., Bris, M.-J. L., Morel, F., & Braekeleer, M. D. (2014). Recurrent translocation (10;17)(p15;q21) in acute poorly differentiated myeloid leukemia likely results in ZMYND11 – MBTD1 fusion. *Leukemia & Lymphoma*, *55*(5), 1189-1190.

Brien, G. L., Gambero, G., O'Connell, D. J., Jerman, E., Turner, S. n. A., Egan, C. M., Dunne, E. J., Jurgens, M. C., Wynne, K., Piao, L., Lohan, A. J., Ferguson, N., Shi, X., Sinha, K. M., Loftus, B. J., Cagney, G., & Bracken, A. P. (2012). Polycomb PHF19 binds H3K36me3 and recruits PRC2 and demethylase NO66 to embryonic stem cell genes during differentiation. *Nature Structural & Molecular Biology*, *19*(12).

Brown, D. T., Wellman, S. E., & Sittman, D. B. (1985). Changes in the Levels of Three Different Classes of Histone mRNA During Murine Erythroleukemia Cell Differentiation. *Molecular and Cellular Biology*, *5*(11), 2879-2886.

Carney, T. J., Dutton, K. A., Greenhill, E., Delfino-Machín, M., Dufourcq, P., Blader, P., & Kelsh, R. N. (2006). A direct role for Sox10 in specification of neural crest-derived sensory neurons. *Development*, *133*(23), 4619-4630. https://doi.org/https://doi.org/10.1242/dev.02668

Chan, A. J. S., Cytrynbaum, C., Hoang, N., Ambrozewicz, P. M., Weksberg, R., Drmic, I., Ritzema, A., Schachar, R., Walker, S., Uddin, M., Zarrei, M., Yuen, R. K. C., & Scherer, S. W. (2019). Expanding the neurodevelopmental phenotypes of individuals with de novo KMT2A variants. *npj Genomic Medicine*, *4*(9). https://doi.org/https://doi.org/10.1038/s41525-019-0083-x

Chasis, J. A., & Mohandas, N. (2008). Erythroblastic islands: niches for erythropoiesis. *Blood*, *112*(3), 470-478. https://doi.org/10.1182/blood-2008-03-077883

Chow, C.-M., Georgiou, A., Szutorisz, H., Silva, A. M. e., Pombo, A., Barahona, I., Dargelos, E., Canzonetta, C., & Dillon, N. (2005). Variant histone H3.3 marks promoters of transcriptionally active genes during mammalian cell division. *EMBO Reports*, *6*(4), 354-360.

Cobben, J. M., Weiss, M. M., Dijk, F. S. v., Reuver, R. D., Kruiff, C. d., Pondaag, W., Hennekam, R. C., & Yntema, H. G. (2014). A de novo mutation in ZMYND11, a candidate gene for 10p15.3 deletion syndrome, is associated with syndromic intellectual disability. *Medical Genetics*, *57*, 636-638.

Coe, B. P., Witherspoon, K., Rosenfeld, J. A., Bon, B. W. M. v., Silfhout, A. T. V.-v., Bosco, P., Friend, K. L., Baker, C., Buono, S., Vissers, L. E. L. M., Schuurs-Hoeijmakers, J. H., Hoischen, A., Pfundt, R., Krumm, N., Carvill, G. L., Li, D., Amaral, D., Brown, N., Lockhart, P. J.,…Eichler, E. E. (2014). Refining analyses of copy number variation identifies specific genes associated with developmental delay. *Nature Genetics*, *46*(10), 1063-1071.

DeScipio, C., Conlin, L., Rosenfeld, J., Tepperberg, J., Pasion, R., Patel, A., McDonald, M. T., Aradhya, S., Ho, D., Goldstein, J., McGuire, M., Mulchandani, S., Medne, L., Rupps, R., Serrano, A. H., Thorland, E. C., Tsai, A. C.-H., Hofstee, Y. H.-., Ruivenkamp, C. A.,…Krantz, I. D. (2012). Subtelomeric Deletion of Chromosome 10p15.3: Clinical Findings and Molecular Cytogenetic Characterization. *Am J Med Genet A*, *158A*(9), 2152-2161.

Detrich, H. W., Kieran, M. W., Chan, F. Y., Barone, L. M., Yee, K., Rundstadler, J. A., Pratt, S., Ransom, D., & Zon, L. I. (1995). Intraembryonic hematopoietic cell migration during vertebrate development. *Proc Natl Acad Sci USA*, *92*(23), 10713-10717. https://doi.org/doi: 10.1073/pnas.92.23.10713

Devoucoux, M., Fort, V., Khelifi, G., Xu, J., Alerasool, N., Galloy, M., Wong, N., Bourriquen, G., Fradet-Turcotte, A., Taipale, M., Hope, K., Hussein, S. M. I., & Côté, J. (2022). Oncogenic ZMYND11-MBTD1 fusion protein anchors the NuA4/TIP60 histone acetyltransferase complex to the coding region of active genes. *Cell Reports*, *39*, 110947.

Ding, Y., & Liu, F. (2022). Protocol for isolation and ATAC-seq library construction of zebrafish red blood cells. *STAR Protocols*, *3*, 101889. https://doi.org/https://doi.org/10.1016/j.xpro.2022.101889

Drane, P., Ouararhni, K., Depaux, A., Shuaib, M., & Hamiche, A. (2010). The death-associated protein DAXX is a novel histone chaperone involved in the replication-independent deposition of H3.3. *Genes and Development*, *24*(12), 1253–1265. https://doi.org/10.1101/gad.566910

Ekblad, C. M. S., Chavali, G. B., Basu, B. P., Freund, S. M. V., Veprintsev, D., Hughes-Davies, L., Kouzarides, T., Doherty, A. J., & Itzhaki, L. S. (2005). Binding of EMSY to HP1b: implications for recruitment of HP1b and BS69. *EMBO Reports*, *6*(7), 675-680.

Ellett, F., Pase, L., Hayman, J. W., Andrianopoulos, A., & Lieschke, G. J. (2011). mpeg1 promoter transgenes direct macrophage-lineage expression in zebrafish. *Blood*, *117*(4), e49-56. https://doi.org/10.1182/blood-2010-10-314120

Elsässer, S. J., Huang, H., Lewis, P. W., Chin, J. W., Allis, C. D., & Patel, D. J. (2012). DAXX envelops a histone H3.3–H4 dimer for H3.3-specific recognition. *Nature*, *491*(7425), 560–565. https://doi.org/10.1038/nature11608

Engel, J. D., Sugarman, B. J., & Dodgson, J. B. (1982). A chicken histone H3 gene contains intervening sequences. *Nature*, *297*, 434-436.

Farrell, J. A., Wang, Y., Riesenfeld, S. J., Shekhar, K., Regev, A., & Schier, A. F. (2018). Single-cell reconstruction of developmental trajectories duringzebrafish embryogenesis. *Science*, *360*(6392). https://doi.org/doi: 10.1126/science.aar3131

Franklin, S. G., & Zweidler, A. (1977). Non-allelic variants of histones 2a, 2b and 3 in mammals. *Nature*, *266*, 273-275.

Fraser, S. T., Isern, J., & Baron, M. H. (2006). Maturation and enucleation of primitive erythroblasts during mouse embryogenesis is accompanied by changes in cell-surface antigen expression. *Blood*, *109*(1), 343-352. https://doi.org/10.1182/blood-2006-03-006569

Ganis, J. J., Hsia, N., Trompouki, E., Jong, J. L. O. d., DiBiase, A., Lambert, J. S., Jia, Z., Sabo, P. J., Weaver, M., Sandstrom, R., Stamatoyannopoulos, J. A., Zhou, Y., & Zon, L. I. (2012). Zebrafish globin switching occurs in two developmental stages and is controlled by the LCR. *Developmental Biology*, *366*, 186-194.

Goldberg, A. D., Banaszynski, L. A., Noh, K.-M., Lewis, P. W., Elsaesser, S. J., Stadler, S., Dewell, S., Law, M., Guo, X., Li, X., Wen, D., Chapgier, A., DeKelver, R. C., Miller, J. C., Lee, Y.-L., Boydston, E. A., Holmes, M. C., Gregory, P. D., Greally, J. M.,…Allis, C. D. (2010). Distinct Factors Control Histone Variant H3.3 Localization at Specific Genomic Regions. *Cell*, *140*, 678-691.

Gore, A. V., Pillay, L. M., Galanternik, M. V., & Weinstein, B. M. (2018). The Zebrafish: A Fintastic Model for Hematopoietic Development and Disease. *Wiley Interdiscip Rev Dev Biol* . *7*(3), e312. https://doi.org/doi:10.1002/wdev.312

Guarnera, L., D'Addona, M., Bravo-Perez, C., & Visconte, V. (2024). KMT2A Rearrangements in Leukemias: Molecular Aspects and Therapeutic Perspectives. *Int. J. Mol. Sci.*, *25*(9023). https://doi.org/https://doi.org/10.3390/ijms25169023

Guo, R., Zheng, L., Park, J. W., Lv, R., Chen, H., Jiao, F., Xu, W., Mu, S., Wen, H., Qiu, J., Wang, Z., Yang, P., Wu, F., Hui, J., Fu, X., Shi, X., Shi, Y. G., Xing, Y., Lan, F., & Shi, Y. (2014). BS69/ZMYND11 Reads and Connects Histone H3.3 Lysine 36 Trimethylation-Decorated Chromatin to Regulated Pre-mRNA Processing. *Molecular Cell*, *56*, 298-310.

Hateboer, G., Gennissen, A., F.M.Ramos, Y., M.Kerkhoven, R., Sonntag-Buckl, V., G.Stunnenberg, H., & Bernards, R. (1995). BS69, a novel adenovirus ElA-associated protein that inhibits EIA transactivation. *EMBO Journal*, *14*(13), 3159-3169.

Hodge, D., Coghill, E., Keys, J., Maguire, T., Hartmann, B., McDowall, A., Weiss, M., Grimmond, S., & Perkins, A. (2005). A global role for EKLF in definitive and primitive erythropoiesis. *Blood*, *107*(8), 3359-3370. https://doi.org/10.1182/blood-2005-07-2888

Howe, K., Clark, M. D., Torroja, C. F., Torrance, J., Berthelot, C., Muffato, M., Collins, J. E., Humphray, S., McLaren, K., Postlethwait, J. H., Nüsslein-Volhard, C., Hubbard, T. J. P., Roest, H., Crollius, Rogers, J., & Stemple, D. L. (2013). The zebrafish reference genome sequence and its relationship to the human genome. *Nature*, *496*(7446), 498–503. https://doi.org/10.1038/nature12111

Jäättelä, M. (1995). Over-expression of hsp70 confers tumorigenicity to mouse fibrosarcoma cells. *Int. J. Cancer*, *60*, 689-693. https://doi.org/https://doi.org/10.1002/ijc.2910600520

Jolly, C., & Morimoto, R. I. (2000). Role of the heat shock response and molecular chaperones in oncogenesis and cell death. *J. Natl, Cancer Inst.*, *92*(19), 1564-1572. https://doi.org/10.1093/jnci/92.19.1564

Kawai, H., Shiraiwa, S., Ogiya, D., Toyosaki, M., Machida, S., Suzuki, R., Onizuka, M., Ogawa, Y., & Kawada, H. (2024). Acute myeloid leukemia with a ZMYND11::MBTD1 fusion gene following chemotherapy and radiotherapy for breast cancer: A case report. *Leukemia Research Reports*, *22*, 100478.

Kim, J.-Y., Kim, K.-B., Eom, G. H., Choe, N., Kee, H. J., Son, H.-J., Oh, S.-T., Kim, D.-W., Pak, J. H., Baek, H. J., Kook, H., Hahn, Y., Kook, H., Chakravarti, D., & Seo, S.-B. (2023). KDM3B Is the H3K9 Demethylase Involved in Transcriptional Activation of lmo2 in Leukemia. *Molecular and Cellular Biology*, *32*(14). https://doi.org/https://doi.org/10.1128/MCB.00133-12

Kingsley, P. D., Malik, J., Fantauzzo, K. A., & Palis, J. (2004). Yolk sac-derived primitive erythroblasts enucleate during mammalian embryogenesis. *Blood*, *104*(1). https://doi.org/10.1182/blood-2003-12-4162

Ladendorff, N. E., Wu, S., & Lipsick, J. S. (2001). BS69, an adenovirus E1A-associated protein, inhibits the transcriptional activity of c-Myb. *Oncogene*, *20*, 125-132.

Lewis, P. W., Elsaesser, S. J., Noh, K.-M., Stadler, S. C., & Allis, C. D. (2010). Daxx is an H3.3-specific histone chaperone and cooperates with ATRX in replication-independent chromatin assembly at telomeres. *PNAS*, *107*, 14075–14080. https://doi.org/10.1073/pnas.1008850107

Li, J., Jr., P. M. G., Gong, W., Storey, A. J., Tsai, Y.-H., Yu, X., Ahn, J. H., Guo, Y., Mackintosh, S. G., Edmondson, R. D., Byrum, S. D., Farrar, J. E., He, S., Cai, L., Jin, J., Tackett, A. J., Zheng, D., & Wang, G. G. (2021). ZMYND11-MBTD1 induces leukemogenesis through hijacking NuA4/TIP60 acetyltransferase complex and a PWWP-mediated chromatin association mechanism. *Nature Communications*, *12*(1045). https://doi.org/https://doi.org/10.1038/s41467-021-21357-3

Liu, C.-P., Xiong, C., Wang, M., Yu, Z., Yang, N., Chen, P., Zhang, Z., Li, G., & Xu, R.-M. (2012). Structure of the variant histone H3.3-H4 heterodimer in complex with its chaperone DAXX. *Nat Struct Mol Biol*, *19*(12), 1287–1292. https://doi.org/10.1038/nsmb.2439

Lu, J., & Gilbert, D. M. (2007). Proliferation-dependent and cell cycle–regulated transcription of mouse pericentric heterochromatin. *The Journal of Cell Biology*, *179*(3), 411–421. https://doi.org/10.1083/jcb.200706176

Luger, K., Mader, A. W., Richmond, R. K., Sargent, D. F., & Richmond, T. J. (1997). Crystal structure of the nucleosome core particle at 2.8A resolution. *Nature*, *389*, 251-260.

Martire, S., Gogate, A. A., Whitmill, A., Tafessu, A., Nguyen, J., Teng, Y.-C., Tastemel, M., & Banaszynski, L. A. (2019). Phosphorylation of histone H3.3 at serine 31 promotes p300 activity and enhancer acetylation. *Nature Genetics*, *52*, 941-946. https://doi.org/https://doi.org/10.1038/s41588-019-0428-5

Masselink, H., & Bernards, R. (2000). The adenovirus E1A binding protein BS69 is a co-repressor of transcription through recruitment of N-CoR. *Oncogene*, *19*, 1538-1546.

McGrath, K. E., Bushnell, T. P., & Palis, J. (2008). Multispectral Imaging of Hematopoietic Cells: Where Flow Meets Morphology. *J Immunol Methods*, *336*(2), 91-97. https://doi.org/10.1016/j.jim.2008.04.012

Millán-Zambrano, G., Burton, A., Bannister, A. J., & Schneider, R. (2022). Histone post-translational modifications — cause and consequence of genome function. *Nature Reviews Genetics*, *23*, 563-580. https://doi.org/https://doi.org/10.1038/s41576-022-00468-7

Mito, Y., Henikoff, J. G., & Henikoff, S. (2005). Genome-scale profiling of histone H3.3 replacement patterns. *Nature Genetics*, *37*(10), 1090-1097.

Musselman, C. A., Avvakumov, N., Watanabe, R., Abraham, C. G., Lalonde, M.-E., Hong, Z., Allen, C., Roy, S., Nuñez, J. K., Nickoloff, J., Kulesza, C. A., Yasui, A., Côté, J., & Kutateladze, T. G. (2012). Molecular basis for H3K36me3 recognition by the Tudor domain of PHF1. *Nat Struct Mol Biol*, *19*(12), 1266-1272.

Palmer, D. K., O'Day, K., Wener, M. H., Andrews, B. S., & Margolis, R. L. (1987). A 17-kD Centromere Protein (CENP-A) Copurifies with Nucleosome Core Particles and with Histones. *The Journal of Cell Biology*, *104*, 805-815.

Paoli, L. D., Cerri, M., Monti, S., Rasi, S., Spina, V., Bruscaggin, A., Greco, M., Ciardullo, C., Famà, R., Cresta, S., Maffei, R., Ladetto, M., Martini, M., Laurenti, L., Forconi, F., Marasca, R., Larocca, L. M., Bertoni, F., Gaidano, G., & Rossi, D. (2013). MGA, a suppressor of MYC, is recurrently inactivated in high risk chronic lymphocytic leukemia. *Leuk Lymphoma*, *54*(5), 1087-1090. https://doi.org/10.3109/10428194.2012.723706

Pevny, L., Lin, C. S., D'Agati, V., Simon, M. C., Orkin, S. H., & Costantini, F. (1995). Development of hematopoietic cells lacking transcription factor GATA-1. *Development*, *121*(1), 163-172. https://doi.org/10.1242/dev.121.1.163

Plesa, A., & Sujobert, P. (2019). Cannibalistic acute myeloid leukemia with ZMYND11-MBTD1 fusion. *Blood*, *133*(16), 1789.

Qian, F., Zhen, F., Xu, J., Huang, M., Li, W., & Wen, Z. (2007). Distinct Functions for Different scl Isoforms in Zebrafish Primitive and Definitive Hematopoiesis. *PLoS Biology*, *5*(5), e132. https://doi.org/doi:10.1371/journal.pbio.0050132

Ravagnan, L., Gurbuxani, S., Susin, S. A., Maisse, C., Daugas, E., Zamzami, N., Mak, T., Jäättelä, M., Penninger, J. M., Garrido, C., & Kroemer, G. (2001). Heat-shock protein 70 antagonizes apoptosis-inducing factor. *Nature Cell Biology*, *3*, 839-843. https://doi.org/https://doi.org/10.1038/ncb0901-839

Ray-Gallet, D., Woolfe, A., Vassias, I., Pellentz, C., Lacoste, N., Puri, A., Schultz, D. C., Pchelintsev, N. A., Adams, P. D., Jansen, L. E. T., & Almouzni, G. (2010). Dynamics of Histone H3 Deposition In Vivo Reveal a Nucleosome Gap-Filling Mechanism for H3.3 to Maintain Chromatin Integrity. *Molecular Cell*, *44*, 928-941. https://doi.org/10.1016/j.molcel.2011.12.006

Renshaw, S. A., Loynes, C. A., Trushell, D. M. I., Elworthy, S., Ingham, P. W., & Whyte, M. K. B. (2006). A transgenic zebrafish model of neutrophilic inflammation. *Blood*, *108*(13), 3976–3978. https://doi.org/https://doi.org/10.1182/blood-2006-05-024075

Ricketts, M. D., Frederick, B., Hoff, H., Tang, Y., Schultz, D. C., Rai, T. S., Vizioli, M. G., Adams, P. D., & Marmorstein, R. (2015). Ubinuclein-1 confers histone H3.3-specific-binding by the HIRA histone chaperone complex. *Nature Communications*, *6*(7711). https://doi.org/10.1038/ncomms8711

Robb, L., Lyons, I., Li, R., Hartley, L., Köntgen, F., Harvey, R. P., Metcalf, D., & Begley, C. G. (1995). Absence of yolk sac hematopoiesis from mice with a targeted disruption of the scl gene. *Proc Natl Acad Sci USA*, *92*(15), 7075-7079. https://doi.org/10.1073/pnas.92.15.7075

Rooij, J. D. E. d., Heuvel-Eibrink, M. M. v. d., Kollen, W. J. W., Sonneveld, E., Kaspers, G. J. L., Beverloo, H. B., Fornerod, M., Pieters, R., & Zwaan, C. M. (2015). Recurrent translocation t(10;17)(p15;q21) in minimally differentiated acute myeloid leukemia results in ZMYND11/MBTD1 fusion. *Genes, Chromosomes, & Cancer*, *55*(3), 237-241. https://doi.org/https://doi.org/10.1002/gcc.22326

Rueb, K. F., & Stachura, D. L. (2021). Using Flow Cytometry to Detect and Quantitate Altered Blood Formation in the Developing Zebrafish. *JoVE Journal of Visualized Experiments*, *170*. https://doi.org/10.3791/61035

Samuels, B. D., Aho, R., Brinkley, J. F., Bugacov, A., Feingold, E., Fisher, S., Gonzalez-Reiche, A. S., Hacia, J. G., Hallgrimsson, B., Hansen, K., Harris, M. P., Ho, T.-V., Holmes, G., Hooper, J. E., Jabs, E. W., Jones, K. L., Kesselman, C., Klein, O. D., Leslie, E. J.,…Chai, Y. (2020). FaceBase 3: analytical tools and FAIR resources for craniofacial and dental research. *Development*, *147*(18), dev191213. https://doi.org/10.1242/dev.191213

Schenk, R., Jenke, A., Zilbauer, M., Wirth, S., & Postberg, J. (2011). H3.5 is a novel hominid-specific histone H3 variant that is specifically expressed in the seminiferous tubules of human testes. *Chromosoma*, *120*, 275-285.

Sullivan, K. E., Hechenberger, M., & Masri, K. (1994). Human CENP-A Contains a Histone H3 Related Histone Fold Domain That Is Required for Targeting to the Centromere. *The Journal of Cell Biology*, *127*(3), 581-592.

Sur, A., Wang, Y., Capar, P., Margolin, G., Prochaska, M. K., & Farrell, J. A. (2023). Single-cell analysis of shared signatures and transcriptional diversity during zebrafish development. *Development Cell*, *58*, 3028-3047. https://doi.org/https://doi.org/10.1016/j.devcel.2023.11.001

Tagami, H., Ray-Gallet, D., Almouzni, G., & Nakatani, Y. (2004). Histone H3.1 and H3.3 Complexes Mediate Nucleosome Assembly Pathways Dependent or Independent of DNA Synthesis. *Cell*, *116*, 51-61.

Tanaskovic, N., Dalsass, M., Filipuzzi, M., Ceccotti, G., Verrecchia, A., Nicoli, P., Doni, M., Olivero, D., Pasini, D., Koseki, H., Sabo, A., Bisso, A., & Amati, B. (2022). Polycomb group ring finger protein 6 suppresses Myc-induced lymphomagenesis. *Life Science Alliance*, *5*(8), e202101344 https://doi.org/https://doi.org/10.26508/lsa.202101344

Tempescul, A., Guillerm, G., Douet-Guilbert, N., Morel, F., Bris, M.-J. L., & Braekeleer, M. D. (2007). Translocation (10;17)(p15;q21) is a recurrent anomaly in acute myeloblastic leukemia. *Cancer Genetics and Cytogenetics*, *172*, 74-76.

Thisse, C., & Thisse, B. (2008). High-resolution in situ hybridization to whole-mount zebrafish embryos. *Nature Protocols*, *3*, 59-69. https://doi.org/https://doi.org/10.1038/nprot.2007.514

Thomsen, M., Ott, F., Loens, S., Kilic-Berkmen, G., Tan, A. H., Lim, S.-Y., Lohmann, E., Schröder, K. M., Ipsen, L., Nothacker, L. A., Welzel, L., Rudnik, A. S., Hinrichs, F., Odorfer, T., Zeuner, K. E., Schumann, F., Kühn, A. A., Zittel, S., Moeller, M.,…Lohmann, K. (2025). Genetic Diversity and Expanded Phenotypes in Dystonia: Insights From Large-- Scale Exome Sequencing. *Annals of Clinical and Translational Neurology*, *0*, 1-12. https://doi.org/https://doi.org/10.1002/acn3.70100

Tober, J., McGrath, K. E., & Palis, J. (2008). Primitive erythropoiesis and megakaryopoiesis in the yolk sac are independent of c-myb. *Blood*, *111*, 2636–2639. https://doi.org/10.1182/blood-2007-11-124685

Tumiene, B., Čiuladaitė, Ž., Preikšaitienė, E., Mameniškienė, R., Utkus, A., & Kučinskas, V. (2017). Phenotype comparison confirms ZMYND11 as a critical gene for 10p15.3 microdeletion syndrome. *Human Genetics*, *58*, 467-474. https://doi.org/10.1007/s13353-017-0408-3

Vargiami, E., Ververi, A., Kyriazi, M., Papathanasiou, E., Gioula, G., Gerou, S., Al-Mutawa, H., Kambouris, M., & Zafeiriou, D. I. (2014). Severe Clinical Presentation in Monozygotic Twins With 10p15.3 Microdeletion Syndrome. *Am J Med Genet Part A*, *164A*, 764–768. https://doi.org/10.1002/ajmg.a.36329

Velasco, G., Grkovic, S., & Ansieau, S. (2006). New Insights into BS69 Functions. *Journal of Biolgical Chemistry*, *281*(24), 16546-16550.

Venkatesh, S., M, S., H, L., MM, G., M, S., S, K., K, N., & JL, W. (2012). Set2 methylation of histone H3 lysine 36 suppresses histone exchange on transcribed genes. *Nature*, *489*, 452-455.

Wei, G., Schaffner, A., Baker, K., Mansky, K., & Ostrowski, M. (2003). Ets-2 interacts with co-repressor BS69 to repress target gene expression. *Anticancer Research*, *23*(3A), 2173-2178.

Wen, H., Li, Y., Xi, Y., Jiang, S., Stratton, S., Peng, D., Tanaka, K., Ren, Y., Xia, Z., Wu, J., Li, B., Barton, M. C., Li, W., Li, H., & Shi, X. (2014). ZMYND11 links histone H3.3K36me3 to transcription elongation and tumour suppression. *Nature*, *508*, 263-281.

Wirbelauer, C., Bell, O., & Schübeler, D. (2005). Variant histone H3.3 is deposited at sites of nucleosomal displacement throughout transcribed genes while active histone modifications show a promoter-proximal bias. *Genes and Development*, *19*, 1761-1766.

Witt, O., Albig, W., & Doenecke, D. (1996). Testis-Specific Expression of a Novel Human H3 Histone Gene. *Experimental Cell Research*, *229*(301-306).

Wu, R. S., Tsai, S., & Bonner, W. M. (1982). Patterns of histone variant synthesis can distinguish G0 from G1 cells. *Cell*, *31*(2), 367-374.

Wunsch, A. M., & Lough, J. (1987). Modulation of histone H3 variant synthesis during the myoblast-myotube transition of chicken myogenesis. *Developmental Biology*, *119*(1), 94-99.

Xu, J., Sankaran, V. G., Ni, M., Menne, T. F., Puram, R. V., Kim, W., & Orkin, S. H. (2010). Transcriptional silencing of γ-globin by BCL11A involves long-range interactions and cooperation with SOX6. *Genes Development*, *24*(8), 783-798. https://doi.org/10.1101/gad.1897310

Yaglom, J. A., Gabai, V. L., & Sherman, M. Y. (2007). High Levels of Heat Shock Protein Hsp72 in Cancer Cells Suppress Default Senescence Pathways. *Cancer Research*, *67*(5), 2372-2381. https://doi.org/doi:10.1158/0008-5472.CAN-06-3796

Yamamoto, K., Yakushijin, K., Ichikawa, H., Kakiuchi, S., Kawamoto, S., Matsumoto, H., Nakamachi, Y., Saegusa, J., Matsuoka, H., & Minami, H. (2018). Expression of a novel ZMYND11/MBTD1 fusion transcript in CD7† CD56+ acute myeloid leukemia with t(10;17)(p 15;q21). *Leukemia & Lymphoma*, *59*(11), 2706-2710.

Yang, C., Wang, K., Liang, Q., Tian, T.-T., & Zhong, Z. (2021). Role of NSD1 as potential therapeutic target in tumor. *Pharmacological Research*, *172*.

Yang, H., Zhang, C., Zhao, X., Wu, Q., Fu, X., Yu, B., Shao, Y., Guan, M., Zhang, W., Wan, J., & Huang, X. (2010). Analysis of copy number variations of BS69 in multiple types of hematological malignancies. *Annals of Hematology*, *89*, 959-964.

Yang, J., Hong, Y., Wang, W., Wu, W., Chi, Y., Zong, H., Kong, X., Wei, Y., Yun, X., Cheng, C., Chen, K., & Gu, J. (2009). HSP70 protects BCL2L12 and BCL2L12A from N-terminal ubiquitination-mediated proteasomal degradation. *FEBS Lett.*, *582*(9), 1409-1414. https://doi.org/10.1016/j.febslet.2009.04.011

Yang, W., & Ernst, P. (2017). Distinct functions of histone H3, lysine 4 methyltransferases in normal and malignant hematopoiesis. *Current Opinion in Hematology*, *24*(4), 322-328. https://doi.org/10.1097/MOH.0000000000000346

Yates, T. M., Drucker, M., Barnicoat, A., Low, K., Gerkes, E. H., Fry, A. E., Parker, M. J., O'Driscoll, M., Charles, P., Cox, H., Marey, I., Keren, B., Rinne, T., McEntagart, M., Ramachandran, V., Drury, S., Vansenne, F., Sival, D. A., Herkert, J. C.,…Balasubramanian, M. (2020a). ZMYND11-related syndromic intellectual disability: 16 patients delineating and expanding the phenotypic spectrum. *Human Mutation*, *41*, 1042-1050. https://doi.org/10.1002/humu.24001

Yates, T. M., Drucker, M., Barnicoat, A., Low, K., Gerkes, E. H., Fry, A. E., Parker, M. J., O'Driscoll, M., Charles, P., Cox, H., Marey, s., Keren, B., Rinne, T., McEntagart, M., Ramachandran, V., Drury, S., Vansenne, F., Sival, D. A., Herkert, J. C.,…Balasubramanian, M. (2020b). ZMYND11-related syndromic intellectual disability: 16 patients delineating and expanding the phenotypic spectrum. *Human Mutation*, *41*, 1042-1050. https://doi.org/DOI: 10.1002/humu.24001

Yi, Z., Cohen-Barak, O., Hagiwara, N., Kingsley, P. D., Fuchs, D. A., Erickson, D. T., Epner, E. M., Palis, J., & Brilliant, M. H. (2006). Sox6 directly silences epsilon globin expression in definitive erythropoiesis. *PLoS Genetics*, *2*(2), e14. https://doi.org/10.1371/journal.pgen.0020014

Yoo, J., Kim, G. W., Jeon, Y. H., Lee, S. W., & Kwon, S. H. (2024). Epigenetic roles of KDM3B and KDM3C in tumorigenesis and their therapeutic implications. *Cell Death and Disease*, *15*(451). https://doi.org/https://doi.org/10.1038/s41419-024-06850-z

Yu, B., Shao, Y., Zhanga, C., Chenc, Y., Zhongb, Q., Zhangb, J., Yang, H., Zhangc, W., & Wan, J. (2009). BS69 undergoes SUMO modification and plays an inhibitory role in muscle and neuronal differentiation. *Experimental Cell Research*, *315*, 3543-3553.

Zang, L., Shimada, Y., Nishimura, Y., Tanaka, T., & Nishimura, N. (2013). A Novel, Reliable Method for Repeated Blood Collection from Aquarium Fish. *Zebrafish*, *10*(00).

Zehtabcheh, S., Samarkhazan, H. S., Asadi, M., Zabihi, M., Parkhideh, S., & Mohammadi, M. H. (2025). Insights into KMT2A rearrangements in acute myeloid leukemia: from molecular characteristics to targeted therapies. *Biomarker Research*, *13*(17). https://doi.org/https://doi.org/10.1186/s40364-025-00786-y

CHAPTER 2

ZMYND11 MODULATES PROLIFERATION AND LINEAGE SPECIFICATION IN ZEBRAFISH PRIMITIVE ERYTHROCYTES

Introduction

The ontogeny of the embryo is a highly complex morphogenetic process characterized by a strong aspect of spatiotemporal order observed similarly in all vertebrates during development. Differentiation of embryonic stem cells into more specialized cell types requires simultaneous activation of differentiation-specific genes and repression of embryonic stem cell–specific genes, which maintain pluripotency and proliferative capacity. Through this coordinated expression of lineage-specific genes, differentiated cell types acquire unique structural and functional traits. Often, dysregulation of these pathways can lead to disease states, such as cancer.

Zmynd11 was first discovered as a transcriptional repressor and was later shown to be a chromatin reader that interacts specifically with trimethylated lysine 36 on Histone H3.3 (H3.3K36me3) through its tandem PHD-BROMO-PWWP chromatin binding domain and recruits several different proteins related to gene regulation, like chromatin remodelers, transcription factors, and splicing-related factors through its C-terminal MYND domain. *ZMYND11* loss of function has been identified in several leukemias, indicating that it normally suppresses proliferation (Yang et al., 2010). A recurrent translocation (10;17)(p15;q21) which creates a fusion protein containing the N-terminus of ZMYND11 and the C-terminus of another protein, MBTD1, has been found in acute myeloid leukemias, that are often minimally or poorly differentiated (Braekeleer et al., 2014; Kawai et al., 2024; Plesa & Sujobert, 2019; Rooij et al.,

2015; Tempescul et al., 2007; Yamamoto et al., 2018) . This mutation is interesting because it replaces the MYND domain of ZMYND11 with MBTD1, which is also a chromatin reader and part of the NuA4 histone acetyltransferase complex. This means that the ZMYND11-MBTD1 fusion protein is presumably still being recruited to target genes containing H3.3K36me3, but instead of recruiting the usual characters with its MYND domain to regulate target gene expression, MBTD1 binding partners, including the NuA4 histone acetyltransferase complex are being aberrantly recruited to ZMYND11 target genes through MBTD1's C-terminus domain. This acetylates and actives transcription of ZMYND11 target genes that would normally be downregulated by ZMYND11's MYND domain binding partners (Devoucoux et al., 2022; Li et al., 2021). Therefore, this fusion protein is not only losing most of ZMYND11's repressive function but also gaining MTBD1's ability to activate expression of genes that would otherwise downregulated. Additionally, patients with ZMYND11 haploinsufficiency report experiencing recurrent infections (Yates et al., 2020b). Taken together, the high rate that *ZMYND11* mutations are found in leukemias along with recurrent infections, strongly suggests that *ZMYND11* plays a role in myeloid lineage specification.

To better understand *zmynd*11's role in blood development, we first studied the phenotypic changes in zebrafish *zmynd11* morphants, followed by the creation of a line of zebrafish carrying a *zmynd11* loss of function mutation. Zebrafish have been used for decades for genetic studies given their high fecundity and transparent embryos, in addition to the fact that zebrafish and humans share approximately 70% of their genes and many cellular processes and pathways are conserved across species (Howe et al., 2013). Similar to humans, zebrafish undergo two waves of blood development, a primitive wave which is formed very early in development and proliferate and mature until around 5 days post fertilization (dpf), which is when the

definitive wave begins to takes over, setting up the hematopoietic stem cell population that supplies the organism with blood cells for the rest of its life. Even though markers for the definitive wave of development, are turned on as early as 32hpf, the vast majority of red blood cells circulating in the first 2-3 days are from the primitive wave (Gore et al., 2018). For developing zebrafish embryos, primitive erythrocyte markers can be seen expressing myeloid and erythrocyte marker in bilateral stripes of the lateral plate mesoderm at about 10-11 hours post fertilization (hpf), then these cells migrate to the primary site of primitive hematopoiesis, the intermediate cell mass (ICM), by about 24hpf and very soon after this primitive erythrocytes enter circulation (Detrich et al., 1995). As red blood cells mature, in zebrafish and mammals, they undergo a series of morphological changes becoming smaller and less granular as they develop (Qian et al., 2007)

Our research shows that *zmynd11* loss of function leads to altered gene expression patterns in red blood cells resulting in increased proliferation and phenotypic changes, like decreased size of red blood cells. Additionally, several genes that play a role in differentiation were dysregulated in *zmynd11* deficient red blood cells, suggesting that *zmynd11*, not only plays a role in suppressing proliferation, but also regulating differentiation of red blood cells.

Materials and Methods

Zebrafish lines and maintenance

All fish were maintained at the University of Georgia. Adults were fed twice a day with Gemma Micro 300 zebrafish food (Skretting, France) and are kept at 28^{o}C with 15 hours light and 9 hours dark. The pH and conductivity of the water was maintained at 6.8-7.2 and 450-550uS, respectively. Embryos were raised at 28^{o}C at a density of 100 embryos per 100mm petri dish.

Morpholino injections

All morpholinos were obtained from Gene Tools, Philomath, OR. Each embryo was injected at the 1-cell stage with 1.6ng *zmynd11* splice blocking morpholino (5'-TGCTCTGGTTTGTGTCTCACCATCT-3') and 2.4ng p53 morpholino. A control mismatched morpholino (misMO) (5'-TACTCTAGTTTATGTCTAACCATAT-3') was also injected into a control group of embryos. One nanoliter of the injection solution, containing 0.05% phenol red (Sigma-Aldrich P-5530) in 0.2M KCl was freshly prepared and injected into the yolk of zebrafish embryos and the embryos were maintained at about 100 embryos per 100cm Petri dish in egg water at 28^{o}C to monitor development over time. Phenol red allows for direct observation of the injected solution in the yolk, and the *zmynd11* morpholino and mismatch morpholino were tagged with a red fluorescent molecule, lissamine, to ensure that morpholino transport from the yolk to the cell pole was complete.

in situ hybridization

Embryos were collected at 4hpf, 24hpf, and 72hpf and fixed overnight with 4% PFA at 4^{o}C, then stored in 100% methanol at -20^{o}C. Whole mount *in situ* hybridization was performed as previously described (Thisse & Thisse, 2008). Gene probes were synthesized using the MEGAscript T7 Transcription Kit (Invitrogen AMB13345), detected with anti-Digoxigenin (DIG)-alkaline phosphatase, Fab fragments (Roche 11093274910) and developed with a mixture of NBT (Thermo 34035) and BCIP (Thermo 34040).

o-dianisidine staining

Dissolve 100mg o-dianisidine powder (Sigma D9143) in 70ml 100% ethanol to make the stock solution at least one day before using because it takes several hours to completely dissolve.

Store at 4°C covered in aluminum foil to protect from light and discard when the solution turns from clear to brown, approximately one month.

48hpf embryos were dechorionated and collected in a 1.7ml Eppendorf tube, 50 embryos per tube. Prepare the working solution fresh each time by mixing the following amounts multiplied by the number of samples: 500µl o-dianisidine stock solution, 125µl 0.1M NaOAc, pH4.5, 500µl sterile water, and 25µl 30% H_2O_2. Without fixing in PFA, add one milliliter of the working solution to each tube of embryos and incubate for 3-5 minutes, monitoring by microscope until the desired amount of amount of staining is achieved. Stop the reaction by rinsing in distilled water three times for 5 minutes and store stained embryos in 4% PFA at 4°C.

CRISPR Cas9 injections to mutate zmynd11 in zebrafish embryos

1-cell WIK embryos were injected into the cell, not the yolk, with 500pg Cas9 RNP and 200pg each of 2 guide RNAs (gRNA) flanking *zmynd11*'s MYND domain to create mosaic mutants: 5'-GGCCATGTACCACTGCTGC-3' and 5'-ATCACAAACGTACCTGCCGC-3'. The Invitrogen MEGAshortscript T7 transcription kit (AM1350) was used to transcribe the gRNAs and Cas9 ribonucleoprotein (RNP) was obtained from PNA Bio Inc. (product number CP01). The offspring of mosaic fish F_o were screened for mutations by extracting genomic DNA at 24 hpf and amplifying the 3'end of *zmynd11* to identify large deletions (Forward 5'-GGTTAACCAAAGCTGCGGAAGTTCAG-3'; Reverse 5'-GCCCTGTTAGCATTCATCGCAACTCAGC-3'). Heterozygous mutants were in-crossed to establish a homozygous population, which were subsequently in-crossed to generate a maternal zygotic mutant population. Genomic DNA was extracted from fin clip specimens of F_1 and F_2 generations followed by PCR of the 3'end of *zmynd11*.

zmynd11 mutant sequencing

A region approximately 400bp in length was PCR amplified with the same primers used for genotyping and purified by adding Agencourt AMPure XP beads (Beckman Coulter A63880) at 0.9X the PCR reaction volume to size select for DNA fragments above 150bp. After washing with 80% ethanol twice, the PCR product was eluted from the beads with 20µl nuclease free water then purity and concentration was checked with both Nanodrop and Qubit. Sanger sequencing was performed by Genewiz.

Western blot

200 zebrafish embryos at 12hpf were deyolked with Ringer's solution (calcium free), with 0.3mM PMSF to inhibit proteases, by pipetting up and down with a 200µl. Rinse once with Ringer's with PMSF and store at -80^{o}C or add lysis buffer and continue with protein quantification. Protein amount was quantified with Pierce BCA Protein Assay Kit (Thermo 23225) and 10µg total protein was added to each well of a Biorad Mini-Protean TGX precast gel (product number 4561084) and subsequently transferred to PVDF membrane (Amersham 10600023). The primary antibody used was ABClonal ZMYND11 rabbit antibody (product number A6327) which targets the N-terminus of ZMYND11 and the secondary antibody used was ABClonal HRP-conjugated Goat anti-Rabbit IgG (H+L) (product number AS014). Each antibody was incubated overnight at 4^{o}C and ECL substrate (Bio-Rad 170-5060) was applied to the membrane and detected with Biorad Gel Doc XR+ set to collect chemiluminescence.

Alcian blue staining

5dpf larvae were fixed overnight in 4% paraformaldehyde in PBS, pH 7.4 at 4^{o}C. After washing three times for five minutes in an acid alcohol (AA) solution made of 70% ethanol (EtOH) and 30% glacial acetic acid (GAA), larvae were stained at room temperature overnight in

a solution of 0.1% alcian blue 8GX (Sigma-Aldrich A5268), 70% EtOH, and 30% GAA. Samples were rinsed several times and differentiated with AA overnight at room temperature. To prepare for dissection, larvae were rehydrated by washing in a series of AA : water for five minutes each (75% AA : 25% water, 50% AA : 50% water, 25% AA : 75% water). After rinsing three times in a saturated sodium borate solution, samples were digested at room temperature in a solution of 1.6% trypsin (Millipore Sigma T4799) in equal parts water and saturated sodium borate. Forceps were used to dissect out the craniofacial cartilage, which were transferred to PBS, pH 7.4 and imaged with a Zeiss Axio Imager.D2.

Creating zmynd11-/-; lcr:GFP zebrafish lines

zmynd11-/- fish were out-crossed with *lcr:GFP* transgenic zebrafish obtained from the Zon lab (Ganis et al., 2012) to create a double heterozygous line (*lcr:GFP* $^{+}$*/- ; zmynd11*$^{+}$*/-*), which were subsequently in-crossed to obtain fish that were *lcr:GFP* $^{+}/_{+}$*; zmynd11-/-*. To identify homozygous *zmynd11* mutants, genomic DNA was extracted from fin clip specimens followed by PCR amplification of the 3'end of *zmynd11*.

Determining the number of mutant and wildtype red blood cells

The protocol for digesting embryos was modified from Rueb and Stachura (2021). For each sample, ten 48hpf embryos were transferred to an Eppendorf tube. The embryos were rinsed once with DPBS (details of recipe), then this was replaced with 500µl DPBS and 6µl 5mg/ml Roche Liberase TM (product number 05401119001) in PBS, pH 7.4 was added to each sample. The Eppendorf tubes were then taped horizontally to the bottom of a shaker set to 185rpm at 37^{o}C and incubated for approximately 45 minutes. Enzyme digestion varies between tubes and must be monitored every few minutes after about 30 minutes to ensure samples are not over-digested. Once digestion is complete, the sample is passed through a 35µm filter into a 5ml

Falcon tube (product number 352235), then 4ml of PBS pH 7.4 with no Ca^{2+} or Mg^{2+} was also passed through the filter to decrease the enzyme's activity. The filter cap was changed to a regular cap and the tubes were centrifuged at 300g for 5 minutes, 4°C to pellet cells. Most of the supernatant was aspirated off, leaving only about 100µl. The total volume was estimated with a pipet then brought up to 300µl with PBS, pH 7.4. 1µl of 1mM thiazole red (Biotium 40087) diluted 1:30 was added to each sample and allowed to incubate at room temperature for 15 minutes to stain dead cells. Samples were analyzed using the Cytek Aurora at the University of Georgia CTEGD Cytometry Shared Resource Laboratory. The gating strategy was as follows: SSC-A vs FSC-A to separate cells from debris → FSC-H vs FSC-A to select for single cells from doublets → GFP vs thiazole red to determine the numbers of GFP-positive red blood cells and dead cells. FlowJo software was used to analyze and compare the number of red blood cells in mutant and wild type embryos.

Hemoglobin qPCR

For each sample, 100 48hpf embryos were collected and separated into 2 Eppendorf tubes, 50 embryos per tube. Embryos were rinsed once with one milliliter ice-cold Ringer's solution (calcium free), then 300µl Ringer's (calcium free) was added and allowed to incubate on ice for 5-10 minutes. Embryos were deyolked by titrating them in and out of a 200µl pipet tip 8-10 times. Deyolked embryos were very briefly centrifuged to pellet the embryos at the bottom of the tube, then the supernatant was removed while avoiding the embryos and large pieces of yolk at the bottom of the tube. The supernatant from 50 deyolked embryos was passed through a 35µm filter into a 5ml Falcon tube (product number 352235), then 700µl PBS, pH 7.4 was also passed through the filter to bring the total volume to one milliliter. Filtering more than the supernatant from 50 embryos into one 5ml tube can result in clumps of cells that are difficult to

completely resuspend, resulting in sample loss. The filter cap was replaced with a regular cap, and the samples were centrifuged at 300g for 5 minutes, 4°C to pellet cells. Most of the supernatant was carefully aspirated with a p1000 pipet, leaving only about 50-100µl of supernatant in the tube to avoid disturbing the cell pellet. The total volume remaining was estimated with a p200 pipet and brought up to 150µl with the addition of PBS, pH7.4, then the cell pellet was resuspended by pipetting up and down 10-15 times. At this point, the supernatant of both tubes was combined, and total RNA was isolated and treated with DNase using Invitrogen's RNAqueous Micro Kit (AM1931).

The primers used to quantify each embryonic hemoglobin gene were previously described in Ganis et. al., 2012. Samples were run on a Roche Lightcycler 480 II (Rotkreuz, Switzerland) with Luna Universal One-Step RT-qPCR Kit Protocol (New England Biolabs E3005) was use for the cDNA synthesis and qPCR reaction. Each sample was run in triplicate and fold change was calculated from the average.

Fluorescence activated cell sorting (FACS) to isolate red blood cells

Total blood cells were obtained in the same way as hemoglobin qPCR, except 350 48hpf embryos were prepared for each sample, 7 tubes of 50 embryos per tube. After deyolking, filtering, and resuspending pelleted cells in PBS, pH 7.4, all seven tubes were combined, and GFP-positive cells were sorted directly into 750µl lysis buffer provided by the Invitrogen RNAqueous Micro Kit (AM1931). Cells were sorted with the Cytek Aurora CS located at the University of Georgia CTEGD Cytometry Shared Resource Laboratory and the FACS gating strategy used was the same as before, when determining the number of red blood cells.

RNA-seq of zmynd11 and wild type isolated red blood cells

After sorting GFP-positive red blood cells, total RNA was isolated using the MicroRNAqueous Kit (Invitrogen AM1931) and treated with DNase (provided with MicroRNAqeous kit) for 30 minutes at 37ºC. Total RNA quality was measured by the Aligent Bioanalyzer. All samples contained about 400ng total RNA with a RIN of at least 8.0. Hemoglobin was depleted using NEBNext RNA Depletion Core Reagent Set (product number E7865) and a pool of ssDNA oligos (2µM each) designed using the NEBNext Custom RNA Depletion Design Tool. The library was prepared using Illumina's stranded mRNA prep, ligation kit (product number 20040532) with Illumina DNA/RNA Unique Dual Indexes Set A (product number 20084067). Messenger RNA was purified from total RNA using poly-T oligo-attached magnetic beads. After fragmentation, the first strand cDNA was synthesized using random hexamer primers followed by second strand cDNA synthesis. The 3' ends were polyadenylated so that adapters could be ligated, followed by amplification of the library. The library was checked with Qubit and Bioanalyzer for size distribution detection. Libraries were pooled and sequenced on Illumina NovaSeq X Plus Series (PE150) by Novagene (Sacramento, CA) to obtain 60 million reads per sample. Reads were aligned to the *Danio rerio* GRCz11 genome using STAR with gene-level counts generated via --quantMode GeneCounts. Differential expression between wild-type and mutant samples was assessed using edgeR following TMM normalization and dispersion estimation. Genes with FDR < 0.05 were considered significant.

Determining the phenotypic characteristics of mutant and wildtype red blood cells

To determine the mean size and granularity of *zmynd11-/-* red blood cells vs wild type, FlowJo software (Ashland, OR) was used to analyze and compare the data collected from sorting

mutant and wild type red blood cells with the Cytek Aurora Cell Sorter (Cytek Biosciences, Fremont, CA).

Results

zmynd11 is expressed in early embryos

We performed zmynd11 in situ on 12hpf, 24hpf, and 72hpf zebrafish embryos to see where *zmynd11* is expressed early in development (Figure 2.1). *zmynd11* is globally expressed in the cell pole at 4hpf but by 24hpf, expression is limited to the head and trunk region. Interestingly, by 72hpf *zmynd11* is still expressed somewhat in the head and also appears to be restricted to the notochord.

zmynd11 morphants exhibit defects in blood and craniofacial development

We wanted to see if interrupting *zmynd11* expression through injection of a splice-blocking morpholino would show phenotypic changes when compared to mismatch injected negative control fish. At 48hpf, blood pooling on the side of the yolk was observed in several morphants. At this stage, zebrafish lie on their side and do not constantly keep themselves upright. When morphants would lie on the same side for a while, the blood would pool on the side gravity favored and little to no blood flow was observed on the top side of the yolk in these embryos. This indicates either a problem with the blood, possibly being more viscous, or with the development of the cardiovascular system that could be functioning at sub-optimal blood pressure and is, therefore, unable to effectively pump blood throughout the body. To better visualize this, o-dianisidine staining was performed at 48hpf on morphants and mismatch controls (Figure 2.2). Moreover, at 5dpf the heart looks enlarged in *zmynd11* morphants (Figure 2.3), but again it is not possible to decipher if the defect is in the blood, cardiovascular system, or both. It's unclear if the heart and/or other components of the cardiovascular system are not

developing correctly or if the blood volume or viscosity is increased and is therefore causing the cardiovascular problems because of the increased demand on the heart to pump harder.

Additionally, when *zmynd11* morpholino is injected into *sox10-GFP* zebrafish (Carney et al., 2006), which express GFP in neural crest derived tissues, craniofacial defects can be seen by 5dpf (Figure 2.4). The lateral view in the top panel shows the craniofacial structures of morphant larvae sloping downward, not upward like the mismatch control. Specifically, the Meckel's cartilage appears to be reduced and more square-shaped in *zmynd11* morphants (bottom panel, red arrow).

Genetically modified zebrafish with zmynd11 loss of function

To try and dissect out if the defect is in the blood or cardiovascular system, we aimed to mutate *zmynd11* in zebrafish. To generate a large deletion in *zmynd11*, zebrafish embryos were injected with Cas9 ribonucleoprotein and two guide RNAs flanking the MYND domain of *zmynd11* (figure 2.5a). Subsequent screening revealed very efficient genome modification with almost all injected fish containing *zmynd11* mutations in their germline. A line of zebrafish was established which contained a 116bp deletion in the *zmynd11* gene, eliminating almost the entire sequence encoding the MYND domain, leaving only 10 bp and the stop codon (Figure 2.5b). An antibody targeting the N-terminus of Zmynd11 was used to check protein expression by western blot and no Zmynd11 protein was detected in the mutant of whole embryo protein extracts at 12hpf (Figure 2.5c). We speculate that this is because the mutation eliminated the 3'splice site for the last exon, which could lead to improper splicing and degradation or may prevent the *zmynd11* transcript from being transported out of the nucleus if it is lacking the polyA tail.

zmynd11/-/- zebrafish larvae exhibit craniofacial defects

Brightfield images of zmynd11-/- larvae at 6dpf show abnormal craniofacial shape as the mouth slopes down, not up as is seen in wild type (Figure 2.6a), which replicated the phenotype observed in *zmynd11* morphant larvae (Figure 2.4a). When we stained 5dpf larvae with alcian blue and dissected out the craniofacial structures, we could see that, like *zmynd11* morphants, the Meckel's cartilage from *zmynd11-/-* larvae was more square-shaped compared to wild type. A superior view shows, the cells of wild type larvae neatly arranged in a row, one cell thick, whereas zmynd11-/- cells are jumbled up and are 2-3 rows thick (Figure 2.6b).

zmynd11 loss of function leads to decreased gata1 expression

gata1 expression is required for red blood cell specification, so we performed *gata1 in situ* hybridization on 12hpf embryos (Figure 2.7). This is about the time that *gata1* expression is first turned on and expression is restricted to the lateral plate mesoderm, which is seen as two stripes running down the length of the body of 12hpf embryos. This revealed decreased *gata1* expression in *zmynd11* mutants, suggesting there could be a problem very early in specifying the blood cell lineages.

zmynd11 loss of function leads to over-proliferation and higher GPF intensity in lcr:GFP red blood cells

Since blood flow defects were observed in *zmynd11* morphants and *gata1* expression was reduced in *zmynd11* mutants, we wanted to better visualize blood flow in live animals. To this end, *zmynd11-/-* fish were crossed with *lcr:GFP* fish, which express GFP under the control of the locus control region (lcr) of globin genes so that red blood cells express GFP (Ganis et al., 2012). Interestingly, by 48hpf, the red blood cells of mutant fish appeared brighter under the fluorescent microscope (Figure 2.8) and persists through at least 7dpf. This prompted the question of

whether there were more red blood cells or if each red blood cell was expressing more GFP. To answer this question, whole embryos at 48hpf were digested by Liberase TM, then flow cytometry analysis was used to quantitate the number of blood cells. Both the *mean* fluorescence intensity and the *median* fluorescence intensity were calculated since the population is not distributed symmetrically (Figure 2.9). The mean fluorescence intensity seems to be standard for calculating fluorescence intensity of individual cells, however the median may be more representative of the population if it is skewed. Results showed that not only were there were more than twice as many red blood cells in mutant fish as wild type, but that the fluorescence intensity of each red blood cell was also significantly increased in the mutants, indicating higher GFP expression.

Embryonic hemoglobin alpha 5 (hbae5) expression is reduced in zmynd11-/- red blood cells

In *lcr:GFP* zebrafish, GFP expression is under the control of the locus control region (lcr) which also regulates expression of hemoglobin genes, so we wondered if hemoglobin expression is altered in zmynd11 mutants since GFP expression appears to be higher. To address this question, we performed qPCR on red blood cells to quantitate expression of the six embryonic alpha- and beta-hemoglobin genes. Interestingly, only embryonic alpha-hemoglobin 5 (*hbae5*) is significantly dysregulated, showing a large reduction in expression in the zmynd11 mutant (Figure 2.10).

Zebrafish red blood cells have different RNA expression profiles

Given that *gata1* and *hbae5* expression is decreased in mutants and GFP seems to be upregulated, we wondered what other genes could be dysregulated in mutant red blood cells, so bulk RNA-seq was used to determine the mRNA profile of mutant red blood cells vs wild type. 48hpf zebrafish were chosen because the definitive wave of blood cell development begins to

enter circulation at 48hpf - 72hpf. Since the primitive and definitive waves originate from different progenitors and have slightly different RNA expression profiles (Farrell et al., 2018; Sur et al., 2023), there is no way to separate the two waves of blood cells once they are in circulation together. Therefore, 48hpf embryos were used to primarily isolate the population of primitive red blood cells.

In zmynd11 mutants, 1705 genes are differentially expressed in primitive red blood cells, with 814 being downregulated and 891 upregulated compared to wild type (Figure 2.11). This was somewhat surprising given *zmynd11's* role in transcriptional repression, until we dug into the data. Several differentially expressed genes are involved in red blood cell differentiation, including key players that control expression of lineage specific markers - *tal1, gata1, runx1t1, fli1, and gfi1ab* (Figure 2.12). *tal1* and *gata1* are transcriptional activators of several genes that are needed to correctly specify red blood cell lineages, and in our *zmynd11* mutant, they are both downregulated, meaning that many of the genes they normally turn on, are probably not adequately expressed, presumably leading to poor differentiation of red blood cells. When we looked at expression of tal1 and gata1 target genes, they were largely downregulated, although not enough to be considered statistically significant. Furthermore, runx1t1, which inhibits the red blood cell transcriptional activator runx1, was downregulated, and another transcriptional repressor, gfi1ab, was also downregulated in mutants, both of which would presumably hinder the ability to adequately inhibit target gene expression and allow proper differentiate. Possibly one of the most imperative proteins for red blood cell identity present of the cell membrane, Rh factor (rhd) is significantly downregulated in mutants, showing that the identity of these cells is being compromised.

Additionally, several transcription factors that are known to have a role in proliferation were dysregulated in zmynd11 mutants, with many of them being upregulated (Figure 2.13) What's even more interesting, is that one of these transcription factors is ETS2, which has been shown to interact with to the MYND domain of zmynd11. In zmynd11 mutants, ETS2 is downregulated, which is interesting because zmynd11 could be directly or indirectly regulating expression of some of its own binding partners. We also looked at expression of some well-established negative regulators of proliferation, including ptenb, mdm2, and cdkn1a (aka p21) and all three were significantly downregulated, suggesting reduced ability to inhibit proliferation.

Furthermore, hsp70 genes are markedly upregulated in *zmynd11-/-; lcr:GFP* primitive erythrocytes, as well as other heat shock proteins that are highly expressed under conditions of stress. (Figure 2.14)

Zmynd11-/- red blood cells are smaller, but show no significant difference in granularity

Given that red blood cells undergo morphological changes as the develop, including a reduction in size and granularity, cell sorting data was analyzed to calculate these parameters in wild type and mutant populations (Figure 2.15). As with fluorescence intensity, both the *mean* and the *median* size (FCS) and granularity (SSC) were calculated since the population is not distributed symmetrically. Interestingly, there was not a significant difference in granularity, however, mutant red blood cells were smaller.

Histograms of cell sorting data reveal unique features of zmynd11-/- blood cells

Overlaying histograms of our sorting data in wild type and zmymd11-/-, shows that mutant red blood cells show a much tighter distribution of GFP intensity, as if all cells are turned up to max, whereas wild type fish have a small population of low GFP intensity, which is missing completely missing in mutant fish (Figure 2.16, black box). In the mutant, there also

appears to be a decrease, although not statistically significant, in GFP-negative cells at the same time there is an increase in GFP-positive cells. It is not known at this time what cell type is decreasing in number, but it would be interesting to know if it's another type of blood cell.

Discussion

This study showed that when *zmynd11* function is lost, primitive erythrocytes over-proliferate and show abnormal phenotypic characteristics, including smaller cell size and blood pooling on the side of the yolk. Our RNA-seq data confirmed that several genes required for lineage specification and proliferation are aberrantly express in *zmynd11-/-; lcr:GFP* primitive red blood cells. The transition from a cell with proliferative capabilities to a cell that has committed to a specific lineage requires an extreme amount of precise gene regulation and changes in the gene expression profile. *zmynd11* seems to help control this transition and in the absence of *zmynd11*, cells continue to proliferate and appear to have problems correctly differentiating into mature erythrocytes. The fact that 12hpf *zmynd11-/-* embryos showed reduced *gata1* expression and it was still reduced in our RNA-seq data at 48hpf, suggests that lineage specific markers may never be adequately expressed to correctly specify lineage. It would be interesting to know if the other genes found to be differentially expressed at 48hpf, are similarly dysregulated at 12hpf, which could indicate that erythrocytes are stuck in a less differentiated state or are developmentally delayed.

Importantly, high expression of heat shock proteins, including *hsp70* and *hsp90*, have been associated with poor cancer prognosis. This is because *hsp70* and *hsp90* normally blocks several steps in the apoptosis pathway, so it is expressed at relatively low levels. However, it has been shown to be overexpressed in several types of cancers (Beer et al., 2002; Jäättelä, 1995; Jolly & Morimoto, 2000) and there's evidence that increased levels of heat shock proteins

protect the cell from apoptosis, leading to increased survival (Ravagnan et al., 2001; Yaglom et al., 2007; Yang et al., 2009). If *zmynd11* loss of function in humans also induces expression of heat shock proteins in cancers, including leukemias, this could be a major factor leading to the poor prognosis associated with *zmynd11* loss of function in leukemia.

As with GFP intensity of *zmynd11-/-; lcr:GFP* red blood cells, they showed a tighter distribution of size and granularity, with less variability in than wild type, suggesting that perhaps the mutant red blood cells are stuck in the same differentiated state, unable to advance to the next stage in development, at least at the same pace as wild type, because of a decrease in cell-type specific gene expression. The smaller cell size relative to wild type would indicate a more differentiated state in wild type, since they get smaller with time, however it is doubtful that cells expressing much lower levels of lineage specific genes would be differentiating faster than their wild type counterparts. Several genes important for cytoskeletal rearrangement and function that are specific to red blood cells, as well as genes required for granularity in myeloid lineages are downregulated. For this reason, size and granularity may not be a good measure of differentiation in zmynd11 red blood cells, because the cells may not sufficiently increase in size and granularity in the first place since the cytoskeleton and granules are probably abnormal compared to wild type.

Although not quite statistically significant, it is worth mentioning the trend observed in our cell sorting data (Figure 2.16). There is a striking difference in peaks when wild type *lcr:GFP* histograms are overlayed with the *zmynd11; lcr:GFP* mutant. The mutant clearly has a higher GFP-positive peak, but what's also interesting is the decrease observed in GFP-negative cells compared to wild type, which among other things would include white blood cells. Keep in mind that the embryos used for these calculations were deyolked, so there are very few cells in

suspension other than blood cells. Further analysis is needed to determine if there is also a decrease in white blood cells, but if this is the case, it seems that *zmynd11* mutants could be making red blood cells at the expense of white blood cells, meaning that without *zmynd11* to help direct lineage specification, the default could be red blood cells.

Moreover, *zmynd11* mutants are missing a small subpopulation of red blood cells with lower GFP intensity (Figure 2.16, black box). This subpopulation was omitted from the sorted cell population used for RNA-seq because it may have skewed the results, but it would be really interesting to know if this subpopulation of cells observed in wild type is perhaps a population of red blood cells that is in a more differentiated state than the majority of red blood cells at 48hpf. This subpopulation could be missing from the *zmynd11-/-; lcr:GFP* red blood cells because specification is delayed in *zmynd11* mutants since necessary genes are not adequately turned on.

Several studies have shown that patients with *ZMYND11* haploinsufficiency experience recurrent infections and *ZMYND11* mutations have been implicated in several types of leukemia. Our research could help explain why patients with *ZMYND11* loss of function mutations have recurrent infections. If *ZMYND11* regulates differentiation of all myeloid lineages, these patients could have poorly differentiated neutrophils and macrophages that are not able to sufficiently react to and fight infections. Understanding how *ZMYND11* functions in blood cell development could lead to the source of how *ZMYND11* loss affects the immune system's ability to fight infection. Additionally, given the relatively high prevalence of *ZMYND11* loss of function in several different types of leukemia, this study will lead to a better understanding of the pathology of *ZMYND11* mutations in cancers. For example, knowing which regulators of proliferation could be dysregulated in *ZMYND11-/-* leukemias, means that drugs like *JUN/FOS* inhibitors

could potentially be used to treat these leukemias to slow proliferation and positively affect patient outcomes.

Finally, it's not clear if the craniofacial defect is a result of over proliferation, aberrant migration, or disorganization of cells, but it the Meckel's cartilage is mishappen in our *zmynd11* mutants. As cell undergo the transition from mesenchyme to cartilage, there is a shift from expressing migratory genes, which allow the cell to travel from the neural tube to the anterior end of the animal, to genes that build and stabilize craniofacial structures. Many of these genes are related to the cytoskeleton and transmembrane receptors that mediate cell adhesion. Looking at the craniofacial phenotype of *zmynd11-/-* larvae (Figure 2.6b), it's not difficult to imagine that there could be a problem with the cytoskeleton and/or cellular adhesion with neighboring cells. In fact, the Meckel's cartilage in *zmynd11-/-* larvae at 5dpf looks very similar to wild type at 3dpf, according to images from Facebase (Samuels et al., 2020), which could mean that craniofacial structures in mutant larvae, specifically Meckel's cartilage, may be stuck in a more immature state, unable to fully express the genes necessary to differentiate and organize properly. It would be interesting to know if these cells are eventually able to properly differentiate and organize, especially since there are not any overtly noticeable craniofacial defects in our *zmynd11-/-* zebrafish once they reach adulthood. Further studies on older larvae are needed to understand if and how the development is delayed or permanently altered.

Figures

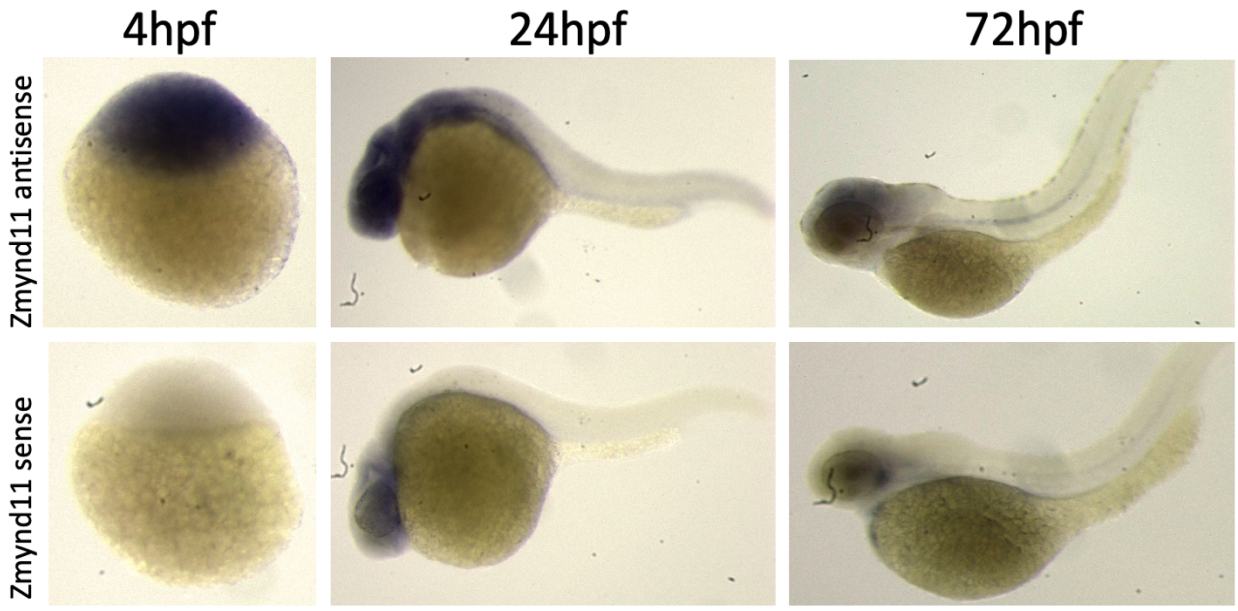

Figure 2.1 *zmynd11* expression at different stages of zebrafish development. *in situ* hybridization was performed on 4hpf, 24hpf, and 72hpf zebrafish using a *zmynd11* sense and antisense probe comprising the full length *zmynd11* cDNA and the complimentary sequence was used as a negative control antisense probe.

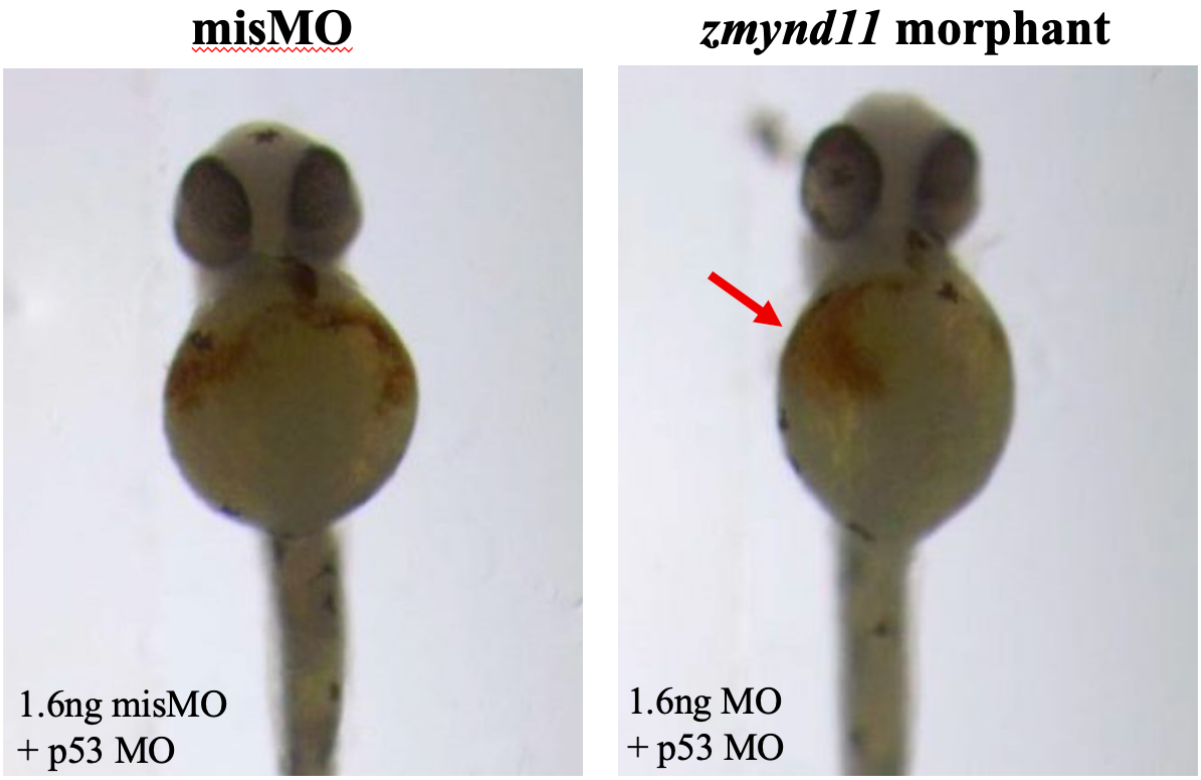

Figure 2.2. *zmynd11* morphants display blood flow defects. Wild type zebrafish were injected with 1.6ng of either *zmynd11* splice-blocking or mismatch (misMO) morpholino. o-dianisidine staining of red blood cells at 48hpf shows defective blood flow in mutants. Red blood cells can be seen pooling on the side of the yolk in morphants (red arrow), whereas wild type embryos show normal blood flow with blood on both sides of the yolk.

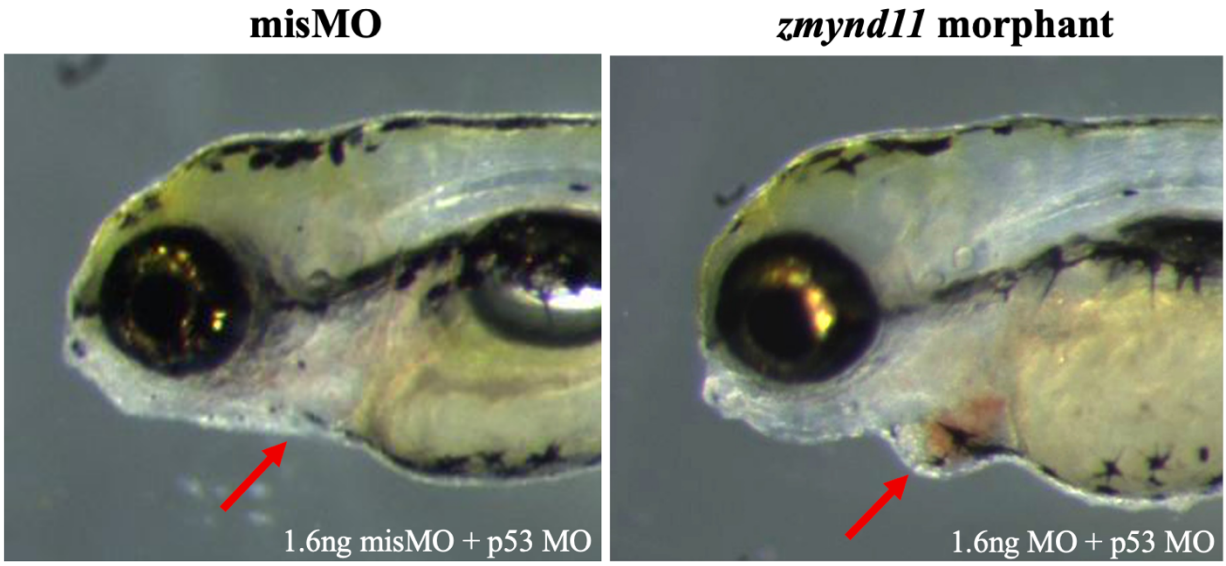

Figure 2.3. Heart/blood defects in *zmynd11* morphants at 5dpf. Zebrafish embryos injected with 1.6ng of either *zmynd11* splice-blocking morpholino or mismatch (misMO) negative control morpholino and development was observed over the first 7 days of development for phenotypic changes. At 5dpf, the heart appears to be enlarged (red arrow).

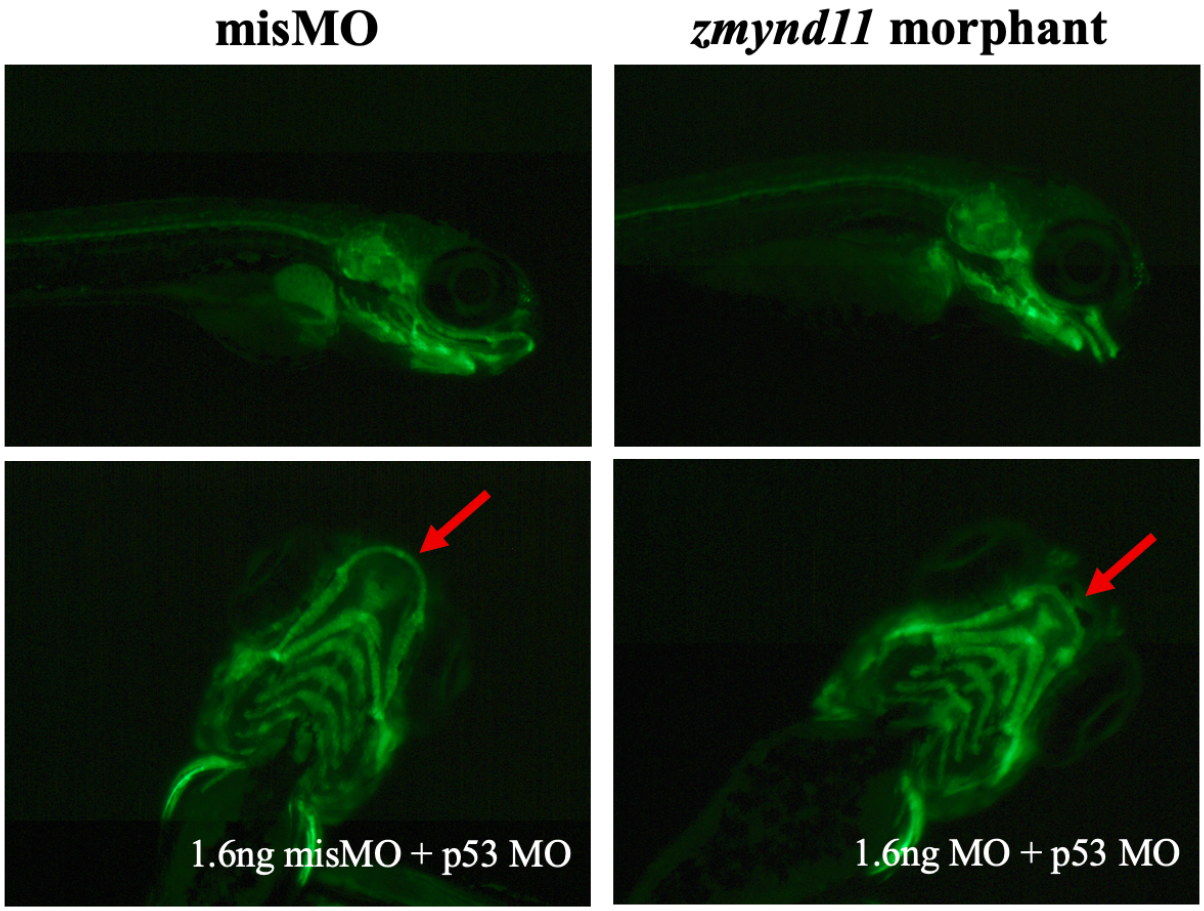

Figure 2.4. Abnormal craniofacial development in *zmynd11* morphants. show at 5dpf. Splice-blocking *zmynd11* morpholino and mismatch morpholino were injected into *sox10-GFP* zebrafish embryos at 1 cell stage and craniofacial structures were observed in whole embryos at 5dfp.

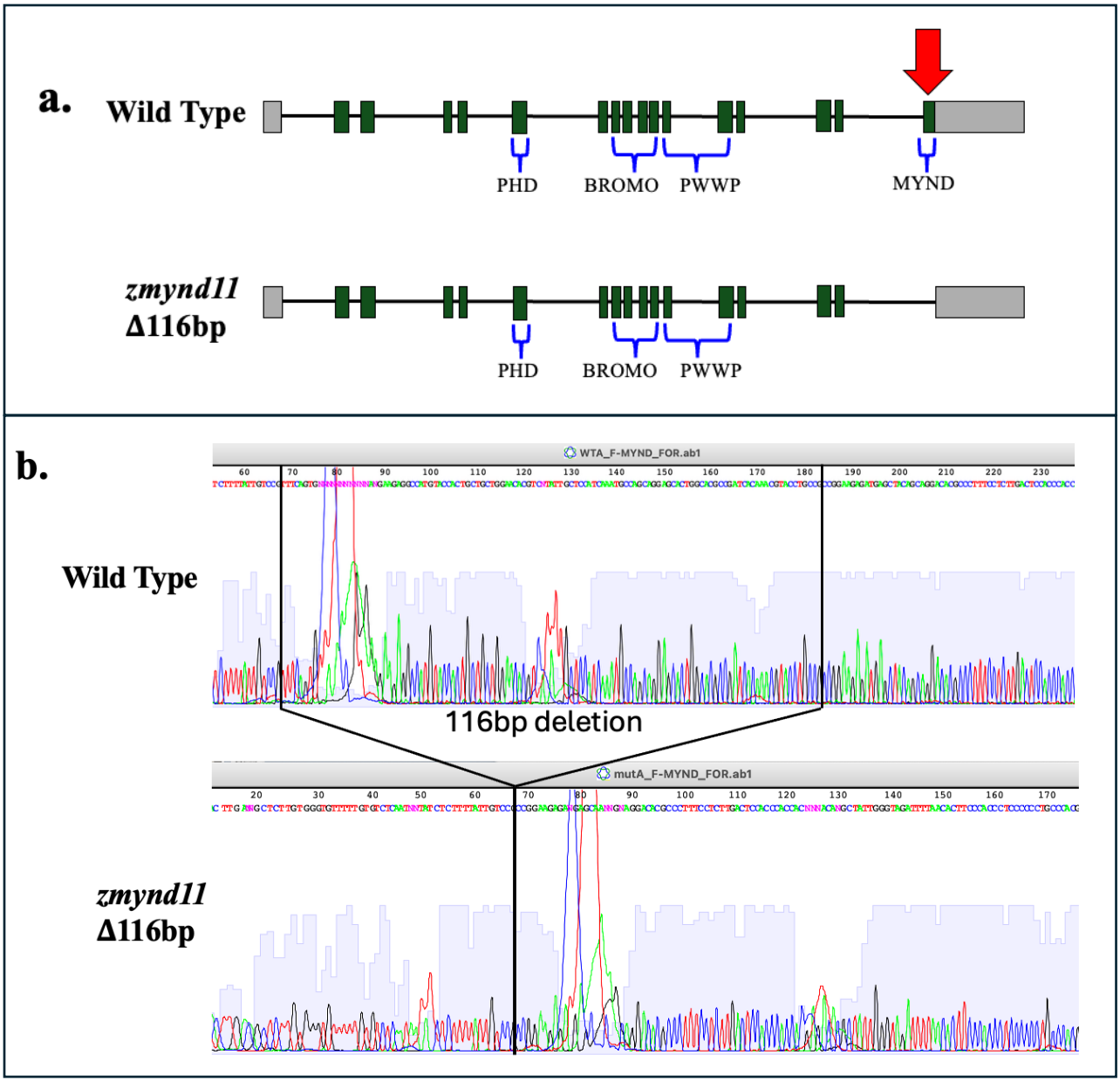

Figure 2.5. Creation of *zmynd11-/-* zebrafish. **(a.)** Diagram of zmynd11 exon organization and the area targeted by gRNAs and CRISPR Cas9 indicated by the red arrow. **(b.)** PCR of the area surrounding the gRNA target sites revealed a large deletion of approximately 116bp, which was confirmed with sequencing **(c.)** *zmynd11* western blot showed no protein product, full length or truncated in the mutant. (Continued on the next page.)

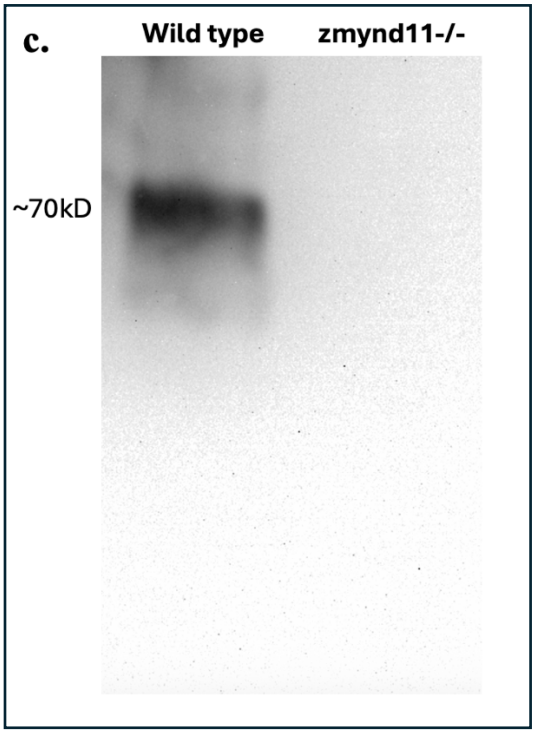
c.
Wild type
zmynd11-/-
~70kD

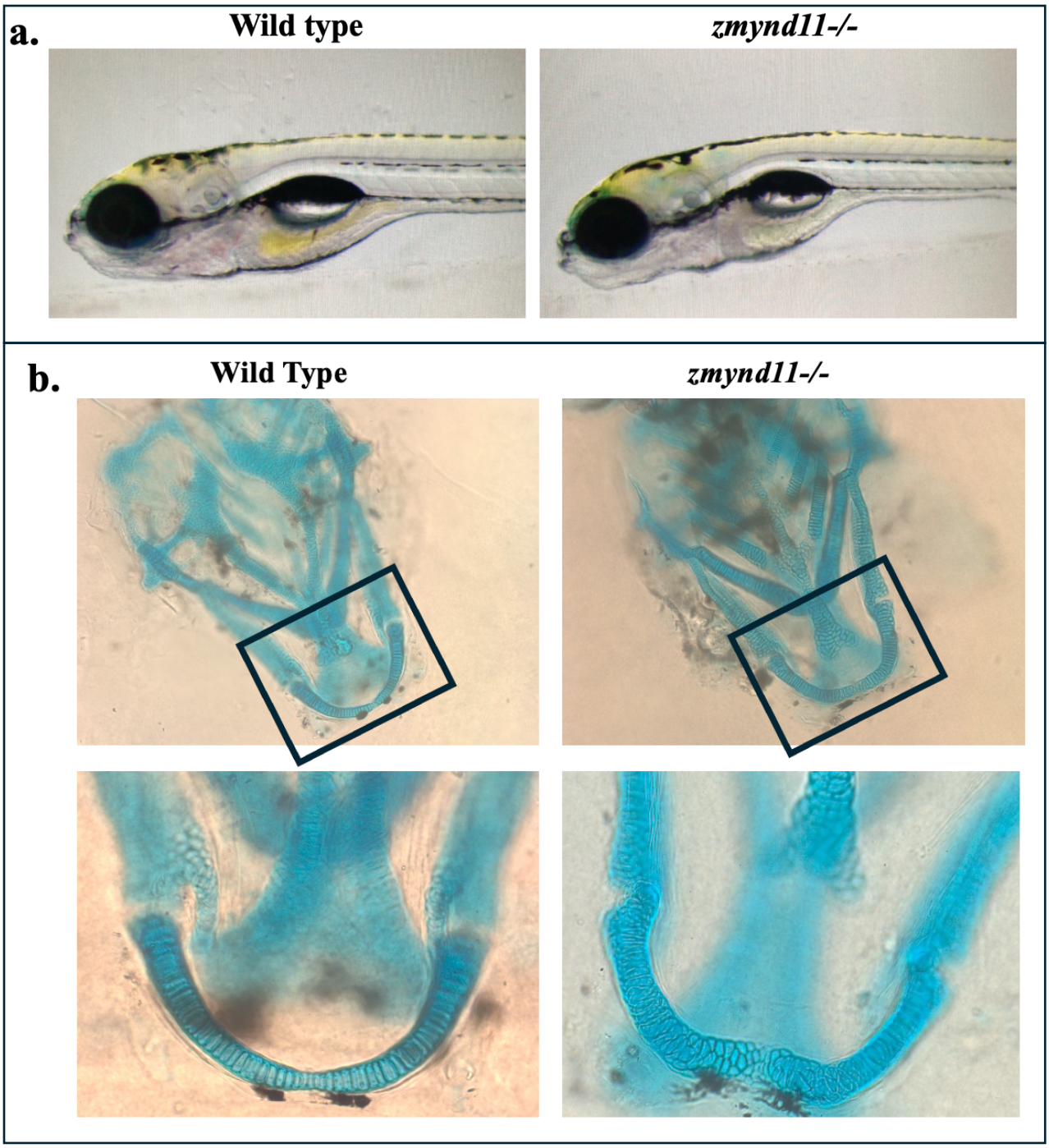

Figure 2.6. Craniofacial defects in *zmynd11-/-* zebrafish. (a.) Brightfield images of wild type and *zmynd11-/-* zebrafish larvae at 6dpf; **(b.)** Alcian blue staining of dissected craniofacial structures in wild type and *zmynd11-/-* zebrafish larvae at 5dpf. A zoomed in image of the region in the black box is shown in the second panel of (b.)

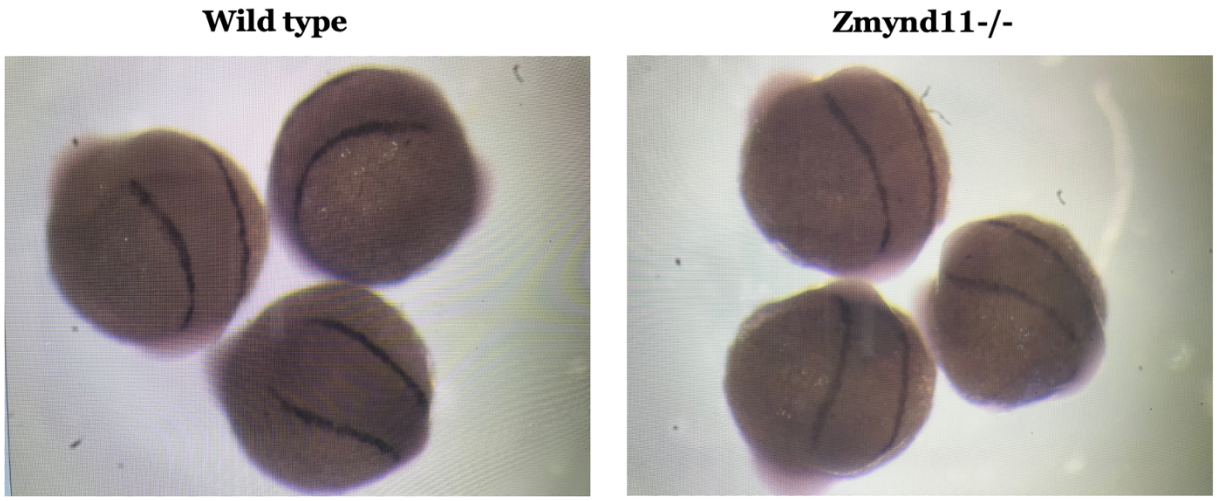

Figure 2.7. *gata1* expression is reduced in zmynd11-/- at 12hpf. *gata1 in situ* hybridization shows decreased expression in *zmynd11-/-* zebrafish compared to wild type.

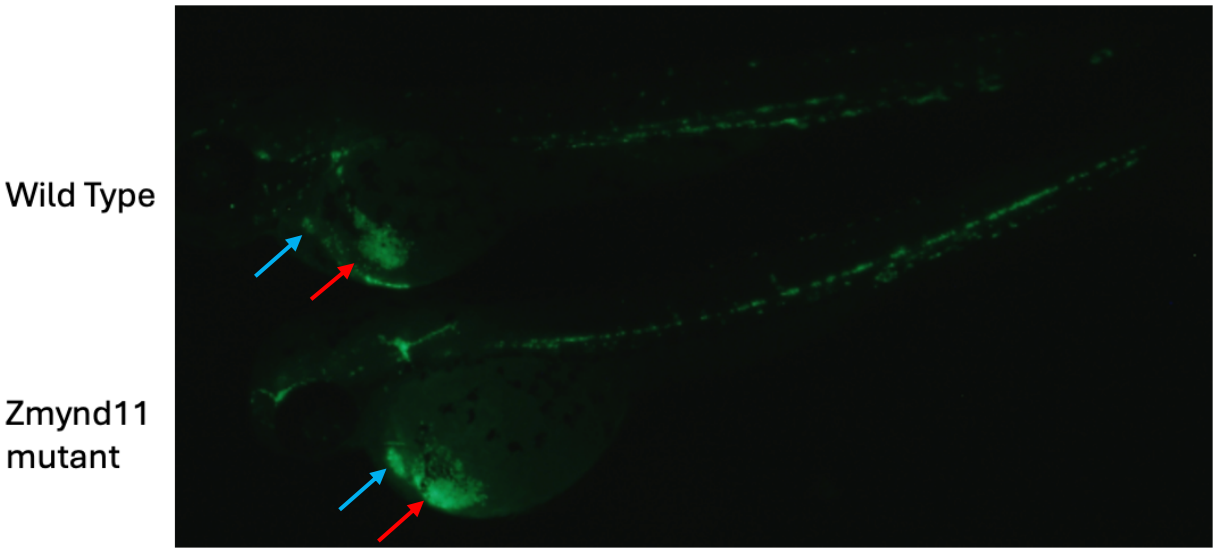

Figure 2.8. *zmynd11-/-; lcr:GFP* red blood cells are visibly brighter. Fluorescent imaging of 48hpf embryos side-by side show the difference in fluorescence, especially noticeable in the heart (blue arrow) and where the blood flows over the yolk (red arrow).

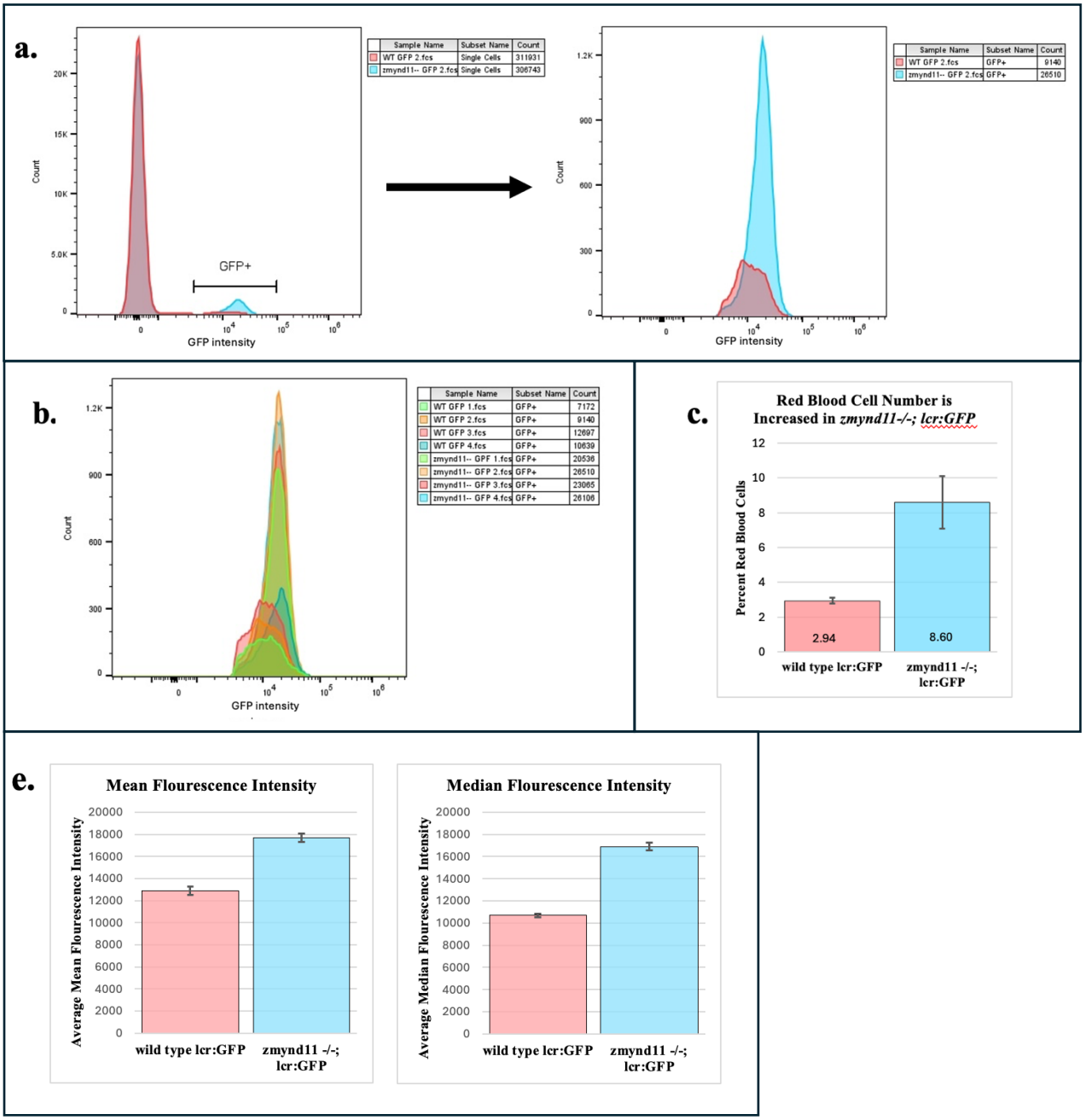

Figure 2.9. *zmynd11 -/-; lcr:GFP* embryos have more red blood cells and increased GFP intensity per cell. Whole embryos were digested with Liberase TM (Roche) and GFP-positive red blood cells were quantitated by flow cytometry. **(a.)** Representative images of flow cytometry analysis results showing a histogram of total single cells (left), then the gated GFP-positive population (right). **(b.)** overlay of the four samples used to calculate the average percentage of red blood cells per embryo. **(c.)** The percentage of GFP-positive cells was quantitated, and the average of four wild type and four mutant samples are show in the graph. **(d.)** The mean and median fluorescence intensity was calculated from the same eight samples used to quantitate GFP-positive cell percentage.

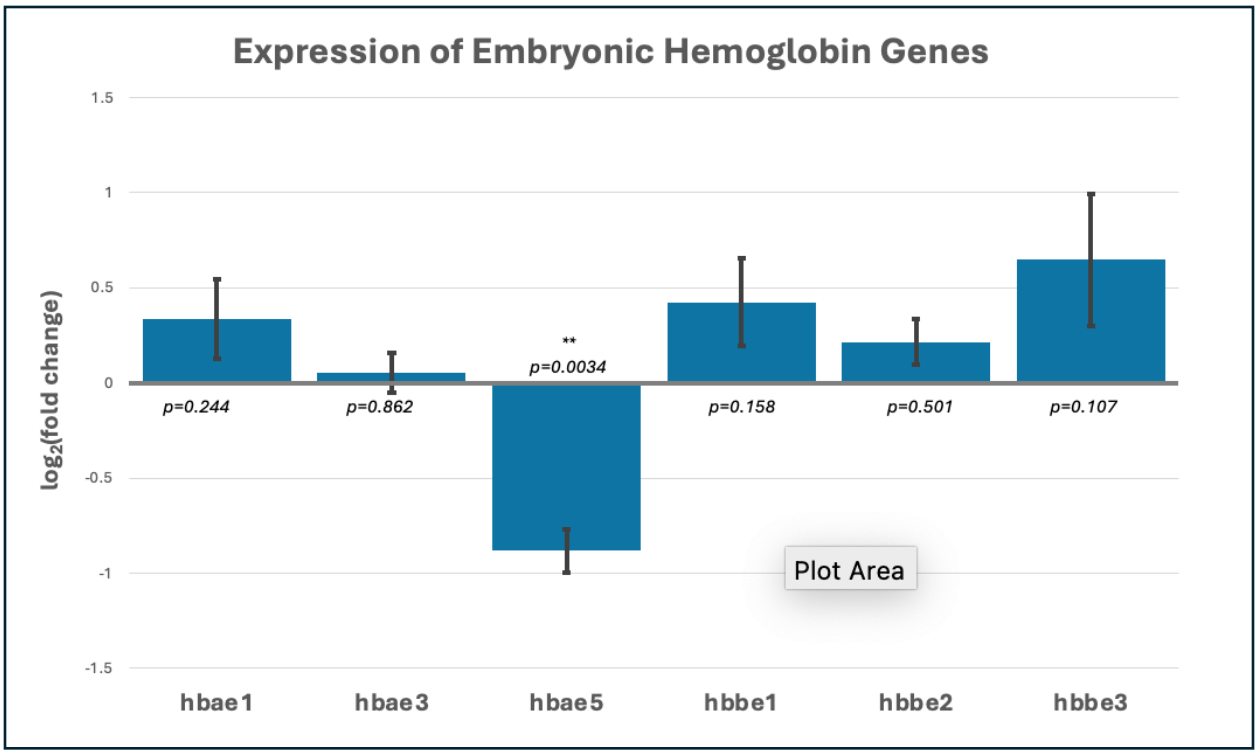

Figure 2.10. Embryonic hemoglobin genes are dysregulated in *zmyndll-/-; lcr:GFP* embryos at 48hpf. Expression levels of embryonic hemoglobin genes in primitive red blood cells of *zmynd11-/-; lcr:GFP* vs *lcr:GFP* wild type at 48hpf were quantified with qPCR. The graph represents the average of four wild type *lcr:GFP* and four *zmynd11-/-; lcr:GFP* samples.

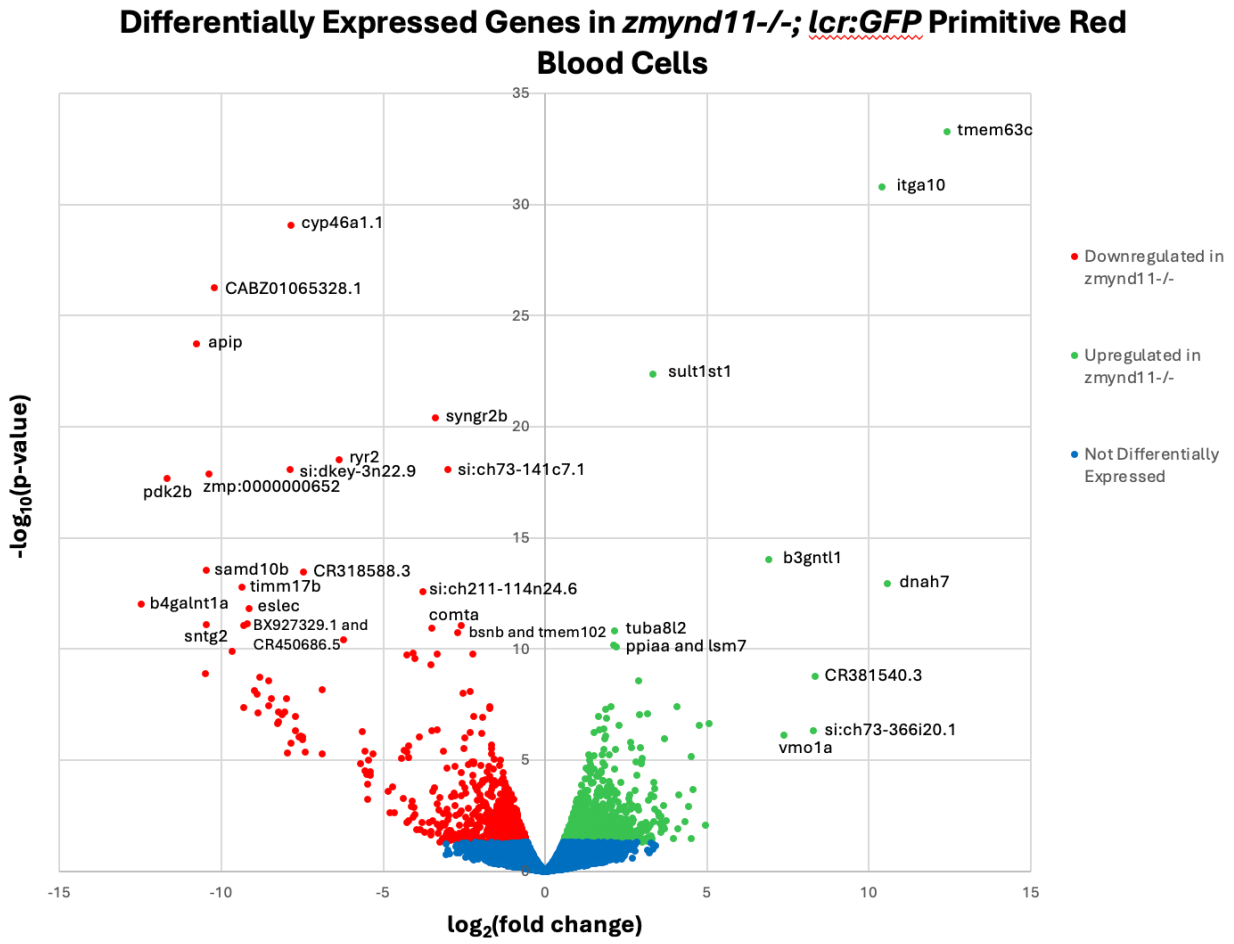

Figure 2.11. Differentially expressed genes in primitive red blood cells of *zmynd11-/-; lcr:GFP* vs wild type *lcr:GFP*. The volcano plot shows genes that are upregulated and downregulated in 48hpf primitive red blood cells of *zmynd11-/-; lcr:GFP* relative to wildtype *lcr:GFP*.

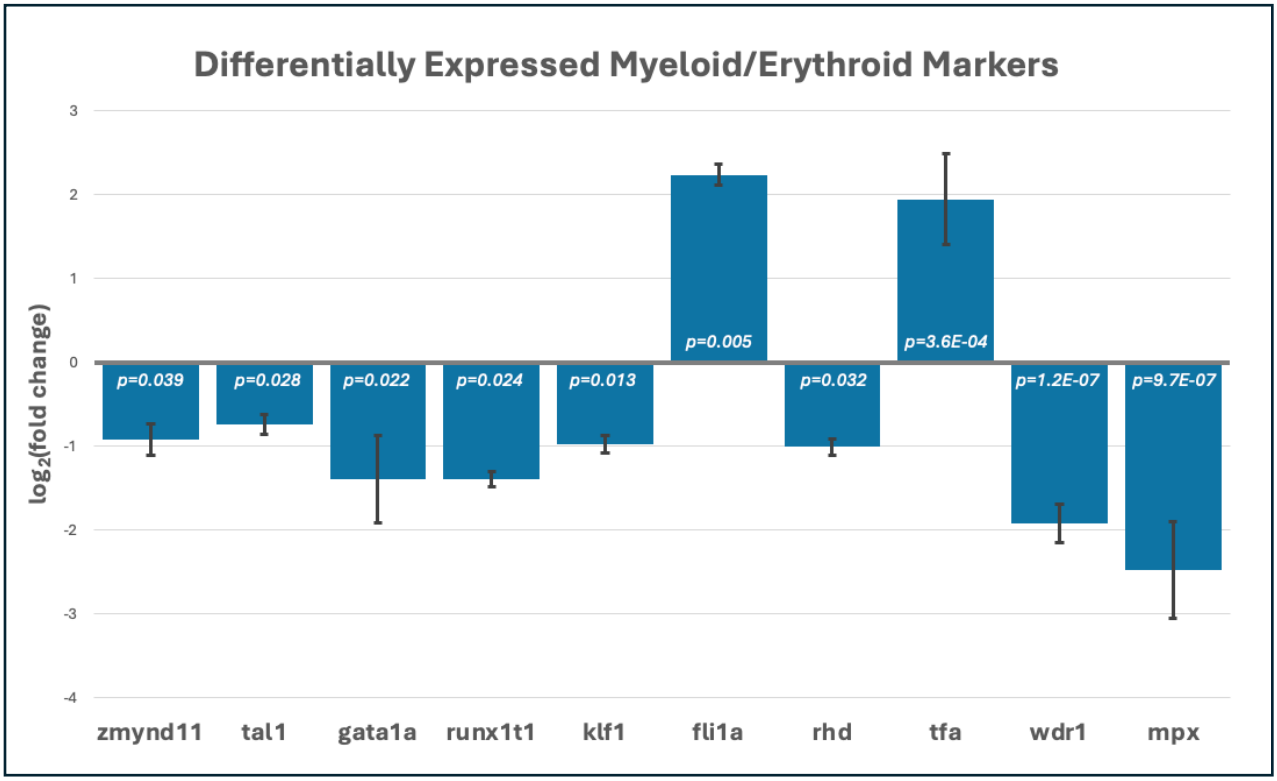

Figure 2.12. Expression of lineage specification markers is dysregulated in *zmynd11-/-; lcr:GFP*. Selected genes are differentially expressed in *zmynd11-/-; lcr:GFP* and are required for proper erythroid specification.

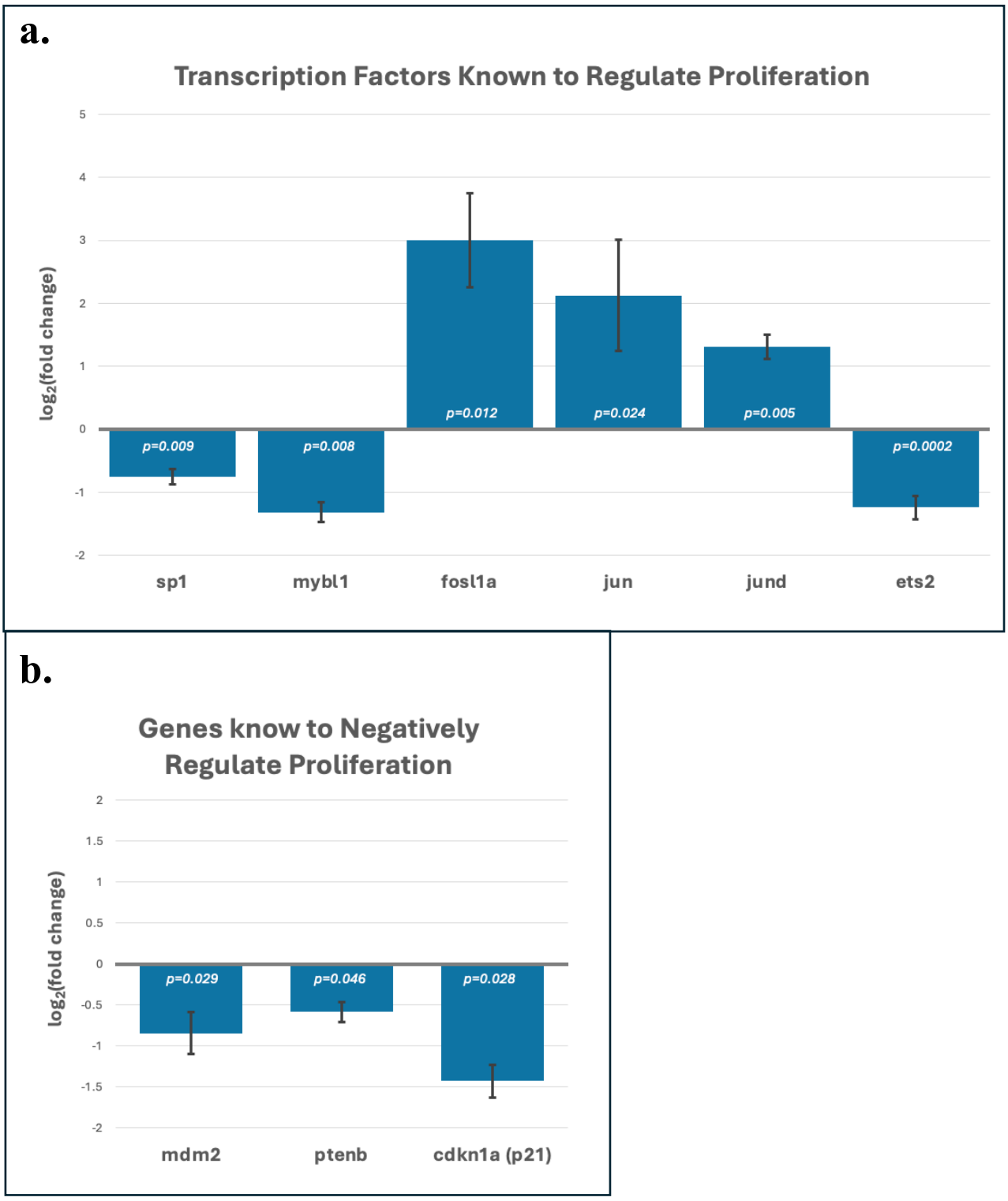

Figure 2.13. Proliferation markers are dysregulated in *zmynd11-/-; lcr:GFP*. **(a.)** Several transcription factors that regulate proliferation are dysregulated in *zmynd11-/ -; lcr:GFP* and **(b.)** three well-known negative regulators of proliferation are significantly downregulated in mutants.

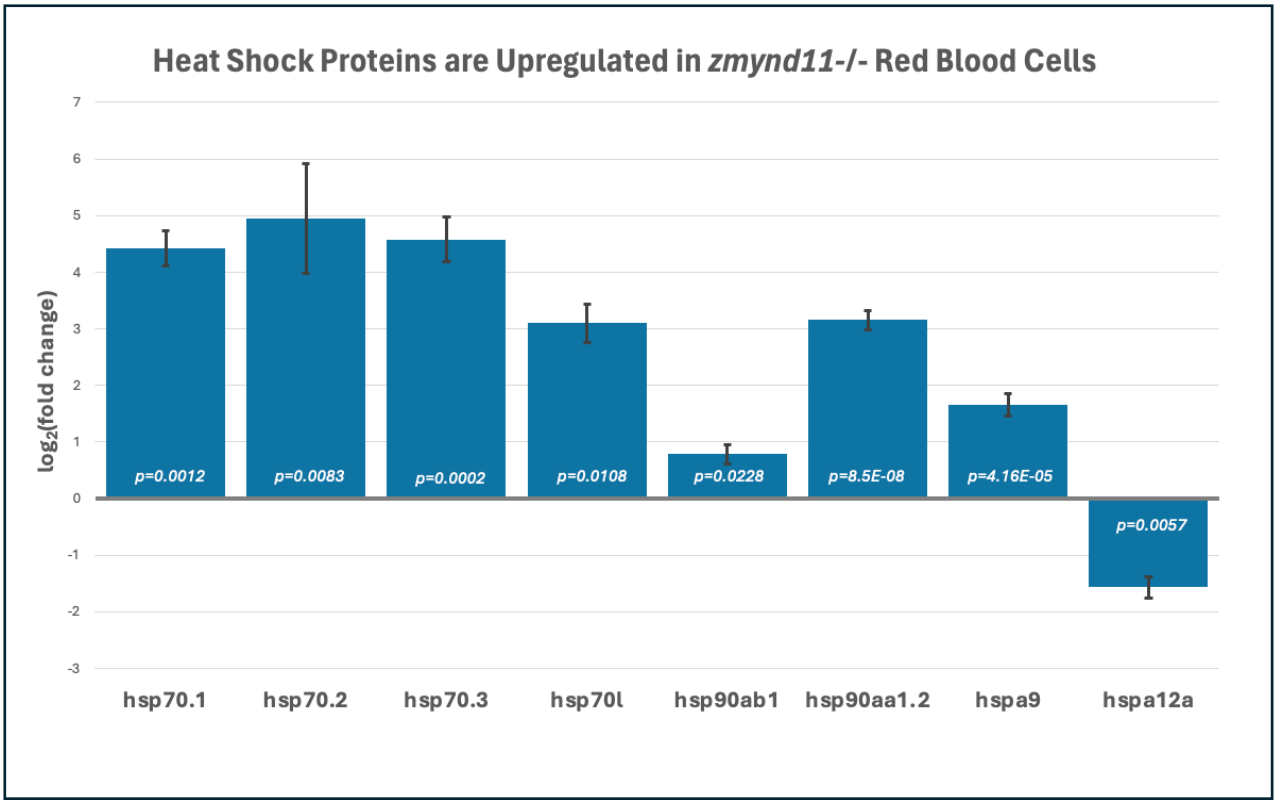

Figure 2.14. Heat shock proteins are dysregulated in *zmynd11-/-; lcr:GFP*. Importantly, *hsp70* and *hsp90* are markedly upregulated in mutant red blood cells.

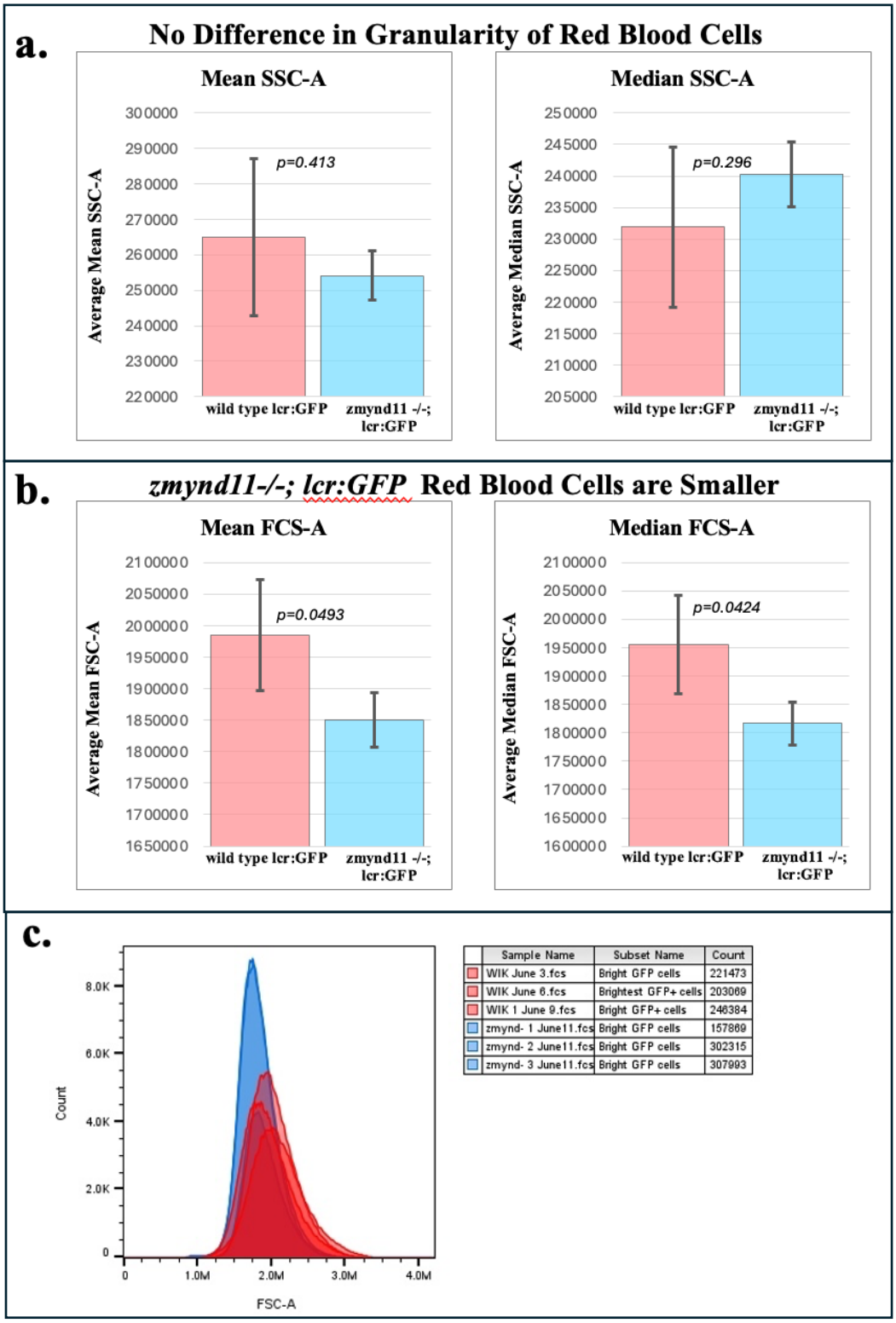

Figure 2.15. *zmynd11-/-; lcr:GFP* red blood cells are smaller than wild type *lcr:GFP*. Comparison of the **(a.)** granularity and **(b.)** size of GFP-positive cells in wild type *lcr:GFP* vs *zmynd11-/-; lcr:GFP* zebrafish at 48hpf. The mean and median of each parameter was calculated since it is an asymmetrical population. **(c.)** A histogram overlaying the size (FSC-A) of three wild type *lcr:GFP* and three *zmynd11-/-; lcr:GFP* samples.

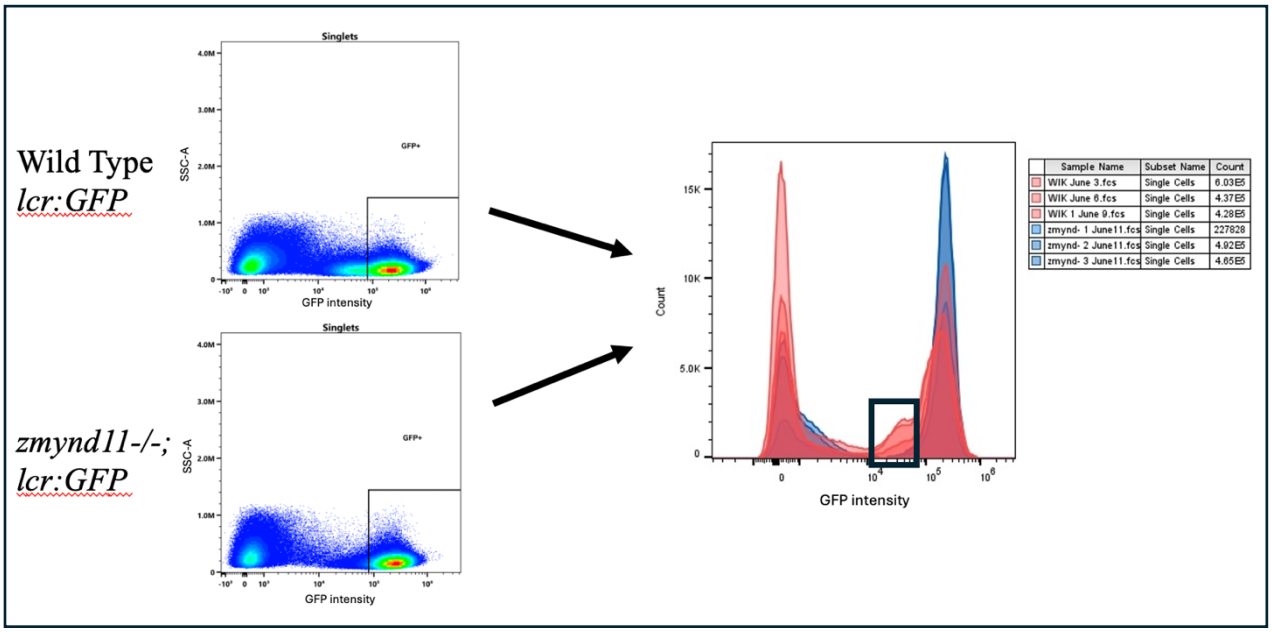

Figure 2.16. Missing subpopulation of GFP-positive cells in sorting data. Representative results of pseudocolor plots (left), which uses color to represent the density of a cell population on a bivariate plot. *Wild type lcr:GFP* shows the presence of subpopulation with GFP intensity from ~10^4-10^5 which is largely absent from *zmynd11-/-, lcr:GFP*. Overlay of three wild type *lcr:GFP* (red) and three *zmynd11-/-; lcr:GFP* (blue) total cell population histograms (right) obtained from cell sorter data. Black box highlights the missing population of cells not seen in *zmynd11-/-; lcr:GFP* mutants.

References

Beer, D. G., Kardia, S. L. R., Huang, C.-C., Giordano, T. J., Levin, A. M., Misek, D. E., Lin, L., Chen, G., Gharib, T. G., Thomas, D. G., Lizyness, M. L., Kuick, R., Hayasaka, S., Taylor, J. M. G., Iannettoni, M. D., Orringer, M. B., & Hanash, S. (2002). Gene-expression profiles predict survival of patients with lung adenocarcinoma. *Nature Medicine*, *8*(8), 816-824. https://doi.org/10.1038/nm733

Braekeleer, E. D., Auffret, R., Douet-Guilbert, N., Basinko, A., Bris, M.-J. L., Morel, F., & Braekeleer, M. D. (2014). Recurrent translocation (10;17)(p15;q21) in acute poorly differentiated myeloid leukemia likely results in ZMYND11 – MBTD1 fusion. *Leukemia & Lymphoma*, *55*(5), 1189-1190.

Carney, T. J., Dutton, K. A., Greenhill, E., Delfino-Machín, M., Dufourcq, P., Blader, P., & Kelsh, R. N. (2006). A direct role for Sox10 in specification of neural crest-derived sensory neurons. *Development*, *133*(23), 4619-4630. https://doi.org/https://doi.org/10.1242/dev.02668

Detrich, H. W., Kieran, M. W., Chan, F. Y., Barone, L. M., Yee, K., Rundstadler, J. A., Pratt, S., Ransom, D., & Zon, L. I. (1995). Intraembryonic hematopoietic cell migration during vertebrate development. *Proc Natl Acad Sci USA*, *92*(23), 10713-10717. https://doi.org/doi: 10.1073/pnas.92.23.10713

Devoucoux, M., Fort, V., Khelifi, G., Xu, J., Alerasool, N., Galloy, M., Wong, N., Bourriquen, G., Fradet-Turcotte, A., Taipale, M., Hope, K., Hussein, S. M. I., & Côté, J. (2022). Oncogenic ZMYND11-MBTD1 fusion protein anchors the NuA4/TIP60 histone acetyltransferase complex to the coding region of active genes. *Cell Reports*, *39*, 110947.

Farrell, J. A., Wang, Y., Riesenfeld, S. J., Shekhar, K., Regev, A., & Schier, A. F. (2018). Single-cell reconstruction of developmental trajectories duringzebrafish embryogenesis. *Science*, *360*(6392). https://doi.org/doi: 10.1126/science.aar3131

Ganis, J. J., Hsia, N., Trompouki, E., Jong, J. L. O. d., DiBiase, A., Lambert, J. S., Jia, Z., Sabo, P. J., Weaver, M., Sandstrom, R., Stamatoyannopoulos, J. A., Zhou, Y., & Zon, L. I. (2012). Zebrafish globin switching occurs in two developmental stages and is controlled by the LCR. *Developmental Biology*, *366*, 186-194.

Gore, A. V., Pillay, L. M., Galanternik, M. V., & Weinstein, B. M. (2018). The Zebrafish: A Fintastic Model for Hematopoietic Development and Disease. *Wiley Interdiscip Rev Dev Biol . 7*(3), e312. https://doi.org/doi:10.1002/wdev.312

Howe, K., Clark, M. D., Torroja, C. F., Torrance, J., Berthelot, C., Muffato, M., Collins, J. E., Humphray, S., McLaren, K., Postlethwait, J. H., Nüsslein-Volhard, C., Hubbard, T. J. P., Roest, H., Crollius, Rogers, J., & Stemple, D. L. (2013). The zebrafish reference genome sequence and its relationship to the human genome. *Nature*, *496*(7446), 498–503. https://doi.org/10.1038/nature12111

Jäättelä, M. (1995). Over-expression of hsp70 confers tumorigenicity to mouse fibrosarcoma cells. *Int. J. Cancer*, *60*, 689-693. https://doi.org/https://doi.org/10.1002/ijc.2910600520

Jolly, C., & Morimoto, R. I. (2000). Role of the heat shock response and molecular chaperones in oncogenesis and cell death. *J. Natl, Cancer Inst.*, *92*(19), 1564-1572. https://doi.org/10.1093/jnci/92.19.1564

Kawai, H., Shiraiwa, S., Ogiya, D., Toyosaki, M., Machida, S., Suzuki, R., Onizuka, M., Ogawa, Y., & Kawada, H. (2024). Acute myeloid leukemia with a ZMYND11::MBTD1 fusion gene following chemotherapy and radiotherapy for breast cancer: A case report. *Leukemia Research Reports*, *22*, 100478.

Li, J., Jr., P. M. G., Gong, W., Storey, A. J., Tsai, Y.-H., Yu, X., Ahn, J. H., Guo, Y., Mackintosh, S. G., Edmondson, R. D., Byrum, S. D., Farrar, J. E., He, S., Cai, L., Jin, J., Tackett, A. J., Zheng, D., & Wang, G. G. (2021). ZMYND11-MBTD1 induces leukemogenesis through hijacking NuA4/TIP60 acetyltransferase complex and a PWWP-mediated chromatin association mechanism. *Nature Communications*, *12*(1045). https://doi.org/https://doi.org/10.1038/s41467-021-21357-3

Plesa, A., & Sujobert, P. (2019). Cannibalistic acute myeloid leukemia with ZMYND11-MBTD1 fusion. *Blood*, *133*(16), 1789.

Qian, F., Zhen, F., Xu, J., Huang, M., Li, W., & Wen, Z. (2007). Distinct Functions for Different scl Isoforms in Zebrafish Primitive and Definitive Hematopoiesis. *PLoS Biology*, *5*(5), e132. https://doi.org/doi:10.1371/journal.pbio.0050132

Ravagnan, L., Gurbuxani, S., Susin, S. A., Maisse, C., Daugas, E., Zamzami, N., Mak, T., Jäättelä, M., Penninger, J. M., Garrido, C., & Kroemer, G. (2001). Heat-shock protein 70 antagonizes apoptosis-inducing factor. *Nature Cell Biology*, *3*, 839-843. https://doi.org/https://doi.org/10.1038/ncb0901-839

Rooij, J. D. E. d., Heuvel-Eibrink, M. M. v. d., Kollen, W. J. W., Sonneveld, E., Kaspers, G. J. L., Beverloo, H. B., Fornerod, M., Pieters, R., & Zwaan, C. M. (2015). Recurrent translocation t(10;17)(p15;q21) in minimally differentiated acute myeloid leukemia results in ZMYND11/MBTD1 fusion. *Genes, Chromosomes, & Cancer*, *55*(3), 237-241. https://doi.org/https://doi.org/10.1002/gcc.22326

Rueb, K. F., & Stachura, D. L. (2021). Using Flow Cytometry to Detect and Quantitate Altered Blood Formation in the Developing Zebrafish. *JoVE Journal of Visualized Experiments*, *170*. https://doi.org/10.3791/61035

Samuels, B. D., Aho, R., Brinkley, J. F., Bugacov, A., Feingold, E., Fisher, S., Gonzalez-Reiche, A. S., Hacia, J. G., Hallgrimsson, B., Hansen, K., Harris, M. P., Ho, T.-V., Holmes, G., Hooper, J. E., Jabs, E. W., Jones, K. L., Kesselman, C., Klein, O. D., Leslie, E. J.,…Chai, Y. (2020). FaceBase 3: analytical tools and FAIR resources for craniofacial and dental research. *Development*, *147*(18), dev191213. https://doi.org/10.1242/dev.191213

Sur, A., Wang, Y., Capar, P., Margolin, G., Prochaska, M. K., & Farrell, J. A. (2023). Single-cell analysis of shared signatures and transcriptional diversity during zebrafish development. *Development Cell*, *58*, 3028-3047. https://doi.org/https://doi.org/10.1016/j.devcel.2023.11.001

Tempescul, A., Guillerm, G., Douet-Guilbert, N., Morel, F., Bris, M.-J. L., & Braekeleer, M. D. (2007). Translocation (10;17)(p15;q21) is a recurrent anomaly in acute myeloblastic leukemia. *Cancer Genetics and Cytogenetics*, *172*, 74-76.

Thisse, C., & Thisse, B. (2008). High-resolution in situ hybridization to whole-mount zebrafish embryos. *Nature Protocols*, *3*, 59-69. https://doi.org/https://doi.org/10.1038/nprot.2007.514

Yaglom, J. A., Gabai, V. L., & Sherman, M. Y. (2007). High Levels of Heat Shock Protein Hsp72 in Cancer Cells Suppress Default Senescence Pathways. *Cancer Research*, *67*(5), 2372-2381. https://doi.org/doi:10.1158/0008-5472.CAN-06-3796

Yamamoto, K., Yakushijin, K., Ichikawa, H., Kakiuchi, S., Kawamoto, S., Matsumoto, H., Nakamachi, Y., Saegusa, J., Matsuoka, H., & Minami, H. (2018). Expression of a novel ZMYND11/MBTD1 fusion transcript in CD7† CD56+ acute myeloid leukemia with t(10;17)(p 15;q21). *Leukemia & Lymphoma*, *59*(11), 2706-2710.

Yang, H., Zhang, C., Zhao, X., Wu, Q., Fu, X., Yu, B., Shao, Y., Guan, M., Zhang, W., Wan, J., & Huang, X. (2010). Analysis of copy number variations of BS69 in multiple types of hematological malignancies. *Annals of Hematology*, *89*, 959-964.

Yang, J., Hong, Y., Wang, W., Wu, W., Chi, Y., Zong, H., Kong, X., Wei, Y., Yun, X., Cheng, C., Chen, K., & Gu, J. (2009). HSP70 protects BCL2L12 and BCL2L12A from N-terminal ubiquitination-mediated proteasomal degradation. *FEBS Lett.*, *582*(9), 1409-1414. https://doi.org/10.1016/j.febslet.2009.04.011

Yates, T. M., Drucker, M., Barnicoat, A., Low, K., Gerkes, E. H., Fry, A. E., Parker, M. J., O'Driscoll, M., Charles, P., Cox, H., Marey, s., Keren, B., Rinne, T., McEntagart, M., Ramachandran, V., Drury, S., Vansenne, F., Sival, D. A., Herkert, J. C.,…Balasubramanian, M. (2020). ZMYND11-related syndromic intellectual disability: 16 patients delineating and expanding the phenotypic spectrum. *Human Mutation*, *41*, 1042-1050. https://doi.org/DOI: 10.1002/humu.24001

CHAPTER 3

AN EFFICIENT METHOD TO ISOLATE PRIMITIVE BLOOD CELLS FROM ZEBRAFISH EMBRYOS FOR DOWNSTREAM APPLICATIONS, SUCH AS RNA-SEQ

Introduction

Zebrafish have been a valuable model organism in developmental biology studies for decades for many reasons. Their short generation time and high fecundity, make it easy to get plenty of embryos which increases reproducibility of data. Additionally, embryos are transparent and develop externally, making zebrafish perfect for studying early embryonic development. Approximately 70% of zebrafish genes have a human ortholog and many of the pathways leading to disease states in humans have an evolutionarily conserved role in zebrafish (Howe et al., 2013). Fortunately, researchers are able to easily inject reagents into developing zebrafish embryos to manipulate target gene expression and study their function. Morpholinos can be used to knockdown gene expression, mRNA injections can overexpress or rescue gene expression, and CRISPR has made it easier than ever to create targeted mutations. Additionally, several GFP-expressing transgenic lines have been created in zebrafish, giving researchers the ability to visualize cell-type specific expression in live organisms over time.

Recent protocols have been developed to quantitate the GFP-positive cell population in zebrafish embryos, by digesting whole embryos and counting the number of cells using flow cytometry (Ding & Liu, 2022; Rueb & Stachura, 2021). However, occasionally experiments warrant the need to isolate these GFP-positive cells, but since blood cells are such a small percentage of total cells in a 48hpf embryo, it would take several hours to isolate enough blood

cells for some downstream applications, such as RNA-seq, making fluorescent-activated cell sorting (FACS) of samples prepared from whole embryo digestion prohibitively expensive and time consuming. For this reason, we have developed a protocol to isolate blood cells expressing a cell-type specific fluorescent reporter protein from zebrafish embryos. Our studies used the *lcr:GFP* line created by the Zon lab (Ganis et al., 2012) to isolate red blood cells, but this method can be used with other reporter lines, including neutrophil- or macrophage-specific lines (Ellett et al., 2011; Renshaw et al., 2006). We specifically chose 48hpf because the embryos almost exclusively have primitive blood cells circulating, with very few blood cells from the early stages of the definitive wave and our goal was to perform RNA-seq on a single cell type to measure differential gene expression in a mutant population vs wild type. 48hpf was also the best time point for this method because the blood cells flow over the yolk to the heart at this time and this protocol releases blood cells into the supernatant by deyolking embryos. However, this procedure could be used at other time points in early development, but the yield of cells sorted will be affected because of the difference in the number of blood cells and the location of blood flow changing in later stages as the yolk shrinks and the blood vessels become closer to the body.

Procedure

1. *Dechorionation of 48hpf embryos*

   Using a transgenic zebrafish line expressing a fluorescent reporter in you cell type of choice, free all embryos from their chorions. By 48hpf many of the embryos have broken themselves out of their chorion, but for those that are not free, forceps or 1mg/ml pronase can be used to dechorionate.

2. *Embryo Collection*

For each sample, separate 350 48hpf embryos into seven 1.7ml Eppendorf tubes, 50 embryos per tube, and place them on ice.

3. Deyolk embryos

Rinse embryos once with one milliliter ice-cold Ringer's solution (calcium free), then 300µl Ringer's (calcium free) was added and allowed to incubate on ice for 5-10 minutes. Embryos were deyolked by titrating them in and out of a 200µl pipet tip 8-10 times.

4. Filter the supernatant containing blood cells

Centrifuge deyolked embryos very briefly centrifuged in a tabletop minicentrifuge for 5 seconds to pellet the embryos at the bottom of the tube. Carefully aspirate the supernatant while avoiding the embryos and large pieces of yolk at the bottom of the tube. Pass the supernatant from 50 deyolked embryos through a 35µm filter into a 5ml Falcon tube (product number 352235), then pass 700µl of PBS pH 7.4 through the filter to bring the total volume to one milliliter. Filtering the supernatant from more than 50-100 embryos into one 5ml tube can result in clumps of cells that are difficult to completely resuspend, resulting in sample loss.

5. Centrifugation to pellet cells

Replace the filter cap with a regular cap and centrifuge the samples at 300g for 5 minutes, 4^{o}C to pellet the cells.

6. Resuspending cells

Carefully, aspirate most of the supernatant with a p1000 pipet, only leaving about 50-100µl supernatant in the tube to avoid disturbing the cell pellet. Estimate the total volume remaining in each tube with a p200 pipet and bring the total volume up to 150µl

with the addition of PBS, pH7.4. Resuspend the cell pellet by pipetting up and down 10-15 times with a p200 pipet. After resuspending all seven tubes, combine them all into one tube.

7. *Fluorescence Activated Cell Sorting (FACS)*

The gating strategy was as follows: SSC-A vs FSC-A to separate cells from debris → FSC-H vs FSC-A to select for single cells from doublets → FSC-H vs GFP (or other fluorescent protein) (Figure 3.1). Depending on the downstream applications, the cells can be sorted into PBS, pH 7.4 or cells can be sorted directly into another appropriate buffer, such as lysis buffer for isolation of RNA, DNA, or proteins.

8. *(Optional) For subsequent RNA-seq experiments on sorted cell population:*
    1. Extract total RNA using Invitrogen RNAqueous Micro Total RNA Isolation Kit (AM1931). Sort cells into 750µl lysis buffer provided in the kit and follow instructions as stated in their protocol.
    2. Following DNase treatment and inactivation (provided with RNA isolation kit), deplete hemoglobin RNA using NEBNext RNA Depletion Core Reagent Set and the pool of DNA oligos in Tables 3.2 and 3.3 at a final concentration of 2µM each.
    3. Proceed with library prep and sequencing.

Representative Results

A simple 3-step gating strategy was used to sort GFP-positive cells. Red blood cells make up 40-75% of the total single cell population in samples prepared by our method, compared to only 6-8% of the total single cell population in whole embryos that have been digested by Liberase TM (Rueb & Stachura, 2021), so the red blood cells are approximately 5-10 times more

enriched using our procedure (Figure 3.1). This is extremely important considering the higher percentage your cell type of interest is, the faster that cell type can be sorted out. In our hands, it would take approximately 5-6 hours to sort 300,000 cells from whole digested embryos, however, we are able to sort that number of cells in only 60-90 minutes using this procedure.

Conclusions

Over the past few decades, zebrafish have become a valuable research tool, especially for developmental studies. Gene expression in zebrafish embryos can be efficiently modified with morpholinos, CRISPR Cas9-directed mutations, or over-expressing injected mRNA. The creation of protocols that help expedite sample preparation through exploitation of embryo anatomy and simple procedures that are standard in the zebrafish community push research forward and highlight how useful zebrafish are when studying developmental processes.

Using this method, we are routinely able to isolate 200,000-300,000 red blood cells from 350 embryos at 48hpf in only about one hour using a Cytek Aurora CS at the University of Georgia CTEGD Cytometry Shared Resource Laboratory. The amount of time needed to prepare samples for sorting was only 1-2 hours per sample, so prepping *and* sorting one sample only takes about 2 to 3.5 hours. Considering this protocol uses a very small amount of easily attainable reagents, with no enzyme incubation period, which first requires tedious optimization of concentration and digestion time, this procedure saves a remarkable amount of time prepping and sorting samples, not to mention the money spent reserving a cell sorter and buying digestion enzymes. Our experiments used a red blood cell reporter, but there is no reason that another reporter line couldn't be used to isolate primitive neutrophils or macrophages from embryos expressing a lineage-specific fluorescent marker for one of these cell types. Additionally,

antibody staining can be used to isolate your cell type of interest if no transgenic line currently exists.

A fluorescent dead cell stain was not added here because we did not see the percentage of dead cells exceed 1% in our initial flow cytometry analysis, so it was not added when sorting because it's such a small population. If there is a high rate of death in your population, it is advisable to use a dead cell stain, but it must have an emission spectrum that does not overlap with the fluorescent signal from the cell type needing to be sorted.

We isolated RNA from our sorted GFP-positive population for RNA-seq experiments, however the procedure described here is also suitable for isolating proteins for western blot, pulldown, mass spectrometry, or chromatin binding experiments, such as CUT N RUN. Depending on the downstream experiments, the sorters available for use should be compared, as we discovered a drastic difference in the concentration and quality of total RNA isolated from cells sorted with different machines. Some cell sorters are gentler and have settings that can be optimized by the user, while others are less adaptable and may not be appropriate for some downstream applications.

Longer sorting times of several hours are difficult logistically because cells begin to die leading to decreased yields, therefore it is imperative find ways to enrich for the population of interest to minimize the time sorting cells, in addition to the money spent reserving a cell sorter. Hopefully, this procedure can help researchers save time and money on their experiments to deliver results as quickly and painlessly as possible.

Figures

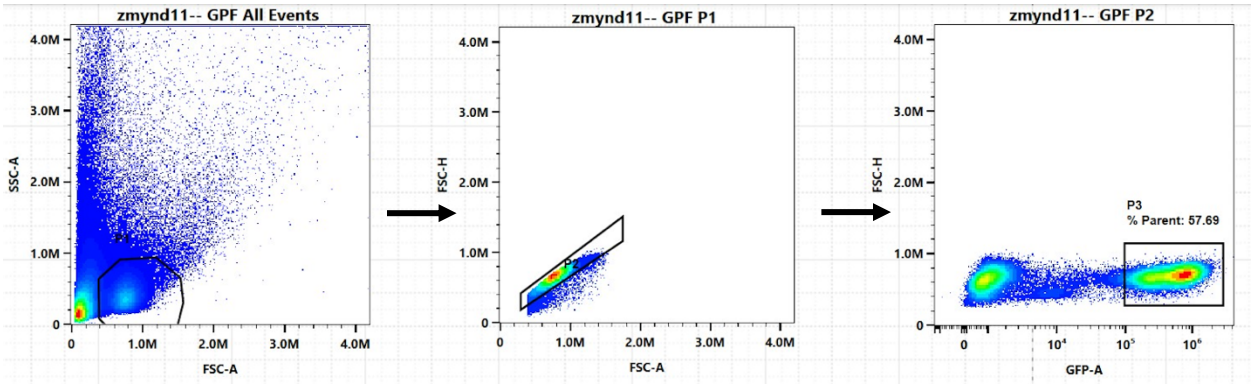

Population Hierarchy
Experiment_014-GFP pos with DSC-zmynd11-- GPF

Population	% Parent	Count
All Events	100.00	308,568
P1	24.45	75,433
P2	96.69	72,933
P3	57.69	42,077

Figure 3.1. Gating strategy for sorting GFP-positive cells with fluorescence activated cell sorting (FACS). The following gating strategy was used to sort out GFP-positive cells: SSC-A vs FSC-A to separate cells from debris → FSC-H vs FSC-A to select for single cells from doublets → FSC-H vs GFP.

Tables

Table 3.1. Consumables needed for sample preparation.

Reagent	**Product Number / Ingredients**
Ringer's (Calcium Free)	82.5mM NaCl 2.5mM KCl 1mM $MgCl_2$ 5mM HEPES
PBS, pH 7.4	137 mM NaCl 2.7 mM KCl 10 mM Na_2HPO_4 1.8 mM KH_2PO_4
Thiazole Red, 1mM (optional)	40087, Biotium
Falcon 5 mL Round Bottom Polystyrene Test Tube, with Cell Strainer Snap Cap	352235

Table 3.2. Sequences of DNA oligos used to deplete embryonic alpha-hemoglobin mRNAs. DNA oligos were designed using NEB's Custom RNA Depletion Design Tool at https://depletion-design.neb.com/

hbae1.1:28-71	CAAACTTCTGTGTCTGAGGCCAGGAGGACAGGCTGTTTTATAC
hbae1.1:58-98	ACTCATTGTGGAAGGATGACTTTACAGCAAACTTCTGTGT
hbae1.1:88-130	GTTTTGACGGCAGCTTTGTCTTTGGCAGAGAGACTCATTGTG
hbae1.1:123-183	AGAGAGCATCGTGTCCGATGTCGTCAGCCTTTCCAGCGATCTTGGCCCACAGGGTTTTGA
hbae1.1:161-203	GTAGACAATCAACATCCTGGAGAGAGCATCGTGTCCGATGTC
hbae1.1:196-256	GCAGAGCCTGGGCTCAGGTCTTTCCAGTGAGAGAAGTAGGTCTTGGTCTGGGGGTAGACA
hbae1.1:228-286	ATCACAGTCTTGCCGTGTTTCCTCACTGGGGCAGAGCCTGGGCTCAGGTCTTTCCAGT
hbae1.1:259-316	ATTTTGCTGACAGCCTCAGCAACGCCTCCCATCACAGTCTTGCCGTGTTTCCTCACT
hbae1.1:294-350	ACTGAGGTTCAGGAGTCCGGCATTAAGGTCATCGATTTTGCTGACAGCCTCAGCAA
hbae1.1:331-371	CAGCTGGAAAGCATGGAGCTCACTGAGGTTCAGGAGTCCG
hbae1.1:375-432	AAGTGGCCAGAACCACGAGGATGTTGTGGGACAGAATCTTGAAATTGGCGGGGTCCA
hbae1.1:407-460	GCCTCAGGAGTGAAATCGGCGGGGAACAAAGTGGCCAGAACCACGAGGATGTT
hbae1.1:439-499	AGAGCCAGAGCTGAGAGGAACTTGTCCATTGCAACATGAGCCTCAGGAGTGAAATCGGCG
hbae1.1:474-514	TTCTCAGACATGGCCAGAGCCAGAGCTGAGAGGAACTTGT
hbae1.1:515-575	AATTTATTGTCTCAATACATAACAGAGAGTTTGGAGCACAGTGAAGTGTGTTTATCTGTA
hbae1.1:560-609	ACACAACAGGCCTTTCGTTAATGTTTTTCATCATAATTTATTGTCTCAA
hbae1.3:458-518	GAATGTTCGTCTGGTTTGACGCGGTTCGACAGGAGCACAGTGAAGTGTGTTTATCTGTAC
hbae1.3:492-542	TATTTATTGCATCACAATAAGACGGAATGTTCGTCTGGTTTGACGCGGTT
hbae3:12-62	CTTGGTTAGCTGTGGGCAGGCTGACAAGAAACTCGAATATTGACAGTTTT
hbae3:53-103	CTTGACGTTCGCTTTGTCCTTTGCGGAAAGACTCATGGTTGCTTGGTTAG
hbae3:85-125	GTGCAACCTTGTCAAAGAAGGCCTTGACGTTCGCTTTGTC
hbae3:127-177	TAAACGAACAAAGTCCTGGAAAGAGTCTCACGGCCGATCTCCTCAGCTTT
hbae3:163-207	CAGTGGGAGAAGTATGTCTTCGTCTGAGGGTAAACGAACAAAGT
hbae3:207-264	TTTATCACCGTGGTTCCGTGCTTCTTCACCTGAGGAGAGTTGGGGCTTAGGTCTGCC

hbae3:238-278	CAGTCAAAACTCCGTTTATCACCGTGGTTCCGTGCTTCTT
hbae3:271-313	CAAACCTCCCTTCAGGTCATCCATCAGCCCGACGGCAGTCAA
hbae3:305-346	CAGCATGAAGGCGTGTAGCTCGCTGAGGGTCAGCAAACCTC
hbae3:375-416	CTGGGAACATCATGGCCAGAGACACCAGCAGATTGTGGTTG
hbae3:337-397	AGACACCAGCAGATTGTGGTTGATGATCTTGAAGTTTGCGGGGTCCACGCGCAGCATGAA
hbae3:451-506	TGCAGCTTTAGCGGTACTTCTCGGACAGGGCCAGGCTGACCTGGGCCAGGAACTT
hbae3:485-538	AATACAGTGTCGCATCAGAGATGAAGGCAGGCTGCAGCTTTAGCGGTACTTCT
hbae3:523-565	TTTATTATTTTCATTCTCATTAAGGCGAATACAGTGTCGCAT
hbae3:553-594	TTTGTTGATTTCATTCAATTTCAATAATATTTATTATTTTC
hbae5:26-76	GAAAGACTCATTTTGAATCGATGTCTGGGATGATCAGACTGGGCACCTAC
hbae5:57-100	CTCACGGCGGCCTTGTCTTTAGCAGAAAGACTCATTTTGAATC
hbae5:91-146	GTTACCAATTTGCTCTCCCTTTGGGGCAATCTTGGCCCAGAAGCCCCTCACGGCG
hbae5:124-175	TACACCAAAAGCAATCTGGAAAACGCCTCGTTACCAATTTGCTCTCCCTTT
hbae5:157-197	GAAGTAGGTCTTGGTCTGAGGGTACACCAAAAGCAATCTG
hbae5:197-255	TCTTCTTTCCCTGCTTCTTCACAGAGGGAGAGCCGGGGGCCAGATCGTTCCAGTGGGA
hbae5:230-289	ATTTTATCAACAGCCAGACCGAGTCCACCGACGATCTTCTTTCCCTGCTTCTTCACAGA
hbae5:261-305	GTTGAAAAGGTCGTCGATTTTATCAACAGCCAGACCGAGTCCAC
hbae5:297-352	TCGACTCTCAGCTGAAAGGCGTGCAATTCACTGAGGTTCAGCAGGCCGTTGAAAA
hbae5:334-384	GACAGTGAGACAGGAGCTTGAAGTTAGCAGGGTCGACTCTCAGCTGAAAG
hbae5:372-422	GAAGTCATCAGGGAAGAGCATGGCGAACACCACCAGCAGACAGTGAGACA
hbae5:411-455	GAACTTGTCGATGGCCAGATGGACCTCAGCGGTGAAGTCATCAG
hbae5:448-498	GTTAACGATATTTGTCAGACAGAGCCAAAGCCACTCTTGCCAGGAACTTG
hbae5:482-532	CGACAAAACCACGTTCATGCTGTTAAACAGAAGAGTTAACGATATTTGTC
hbae5:519-561	TGTTTTTATTGACATGCTGTTGACCATATCGACAAAACCACG

Table 3.3. Sequences of DNA oligos used to deplete embryonic beta-globin mRNAs. DNA oligos were designed using NEB's Custom RNA Depletion Design Tool at https://depletion-design.neb.com/

hbbe1.1:43-103	GATATCTTGAATGGTGGCCTTCTCGAAGTCTGTCCACACAACCATGTTTTCGACTTTAGA
hbbe1.1:466-526	ATTATAATCTCTCTCTGTCTGTATTTAGTGGTACTGTCTTCCCAGAGCGGACACGGCGAC
hbbe1.1:75-135	GGACCGATGACGTCGTAGTCAGCCTTGGCGAAGATATCTTGAATGGTGGCCTTCTCGAAG
hbbe1.2:418-478	GGACACCGCAACAGCGATGAATTTCTGGAAAGCGGCCTGAACTTCAGGTGTGAATCCAGC
hbbe1.3:237-297	TCCATGTTCTTCACTGCCAGCTCCAGACCTTTGAGCACAGTTTTACCGTGGGCAGCAACC
hbbe1.3:279-339	GAGTGCAGCACACTCAAATCAGCATAGGTGGCCTTGATGTTGTCCATGTTCTTCACTGCC
hbbe2:26-86	CGCAACCATGTTGTTGATTTATGATTTTCTTCTCTGTCAAGAACAAGAATCATACCTTTG
hbbe2:334-394	AGCCTGAAGTTGTCAGGATCCACGTGCAGTTTCTCGGAGTGCAGCACGCTCAGCTCGGCG
hbbe3:367-427	AACAACAGACAGGAACTTCTGCCAAGCAGCTTGGATGTCCGGGGTGAACTCACTCCTCAT
hbbe2:453-511	TGTCTTTGCAGAGCAGAGACAACAACAGCGAGGAACTTCTGCCAGGCAGCCTGCATGT
hbbe2:128-185	ATACACAATCAAAGCCCTCTGCAGTGCTTTGGGTCCAGCCTCCTCATAGTTGAGTTT
hbbe2:271-328	TTCTTGATGTCATCCATGTTCTTCATGGCTCTGTCCAGTCCGTGGAGCACGACGGTT
hbbe3:64-121	ATAGACGACCAAGCATCTTGTCAAGGTCTCGAGGCCCACCGACTCAAAGTCGAGTTT
hbbe1.2:527-583	TGAATAGTGAAATATTTATTTGCTTCAACTCAGAATAGCACATTCTTTAGTGGAAA
hbbe1.3:205-261	ACAGTTTTACCGTGGGCAGCAACCATTGGGTTTCCCAGGATGGCAGCGGCATTGTA
hbbe3:120-176	TTGCCTCTGTGTTGTATAGGTTTCCAAACCCACCAAAGTACCGCTGAGTCCACGGA
hbbe3:401-456	TAAAGATATTGCCTTCTGAGGGCTGACACAACAACAGACAGGAACTTCTGCCAAG
hbbe2:58-112	ATGAAGGCACGTTCCTCGGCGGTCCACGCAACCATGTTGTTGATTTATGATTTT
hbbe2:523-575	TTTATTGCGTTTGAGAGCAAACATACAATGTTTCCCCACCACATCTGAGAGG
hbbe1.1:353-403	AACAACGATGGTCAAGCAATCAGCCAAAAGCCTGAAGTTGTCGGGATCTA
hbbe1.2:22-72	GTCCACACAACCATGTTTTCGACTTTAGATGTTCAGACTAAGTGTCTTAA
hbbe2:169-219	TTCCAAAACTTCCAAAGTATCTCTGAGTCCAGGGATACACAATCAAAGCC

hbbe2:207-257	CTTTGGGTTGTTAATGATGGCCTCAGCATTGTACAGGTTTCCAAAACTTC
hbbe2:485-535	ACATCTGAGAGGTCTTAATGATACTGTCTTTGCAGAGCAGAGACAACAAC
hbbe3:220-270	TAGGTGCTCTTGATATTATCCATGTTGTTGAGAGCCTTTTCAAGTCCCTT
hbbe3:251-301	TTTCTCTGAGTGAAGCTCGCTGAGAGAAGCATAGGTGCTCTTGATATTAT
hbbe3:29-79	CTCAAAGTCGAGTTTGGCAAAGATGTTCTGAATCGCTGCGCGCTCCTCAG
hbbe3:433-483	ACAATCACTTCTTTCGGTAAGCGAATCTAAAGATATTGCCTTCTGAGGGC
hbbe2:374-423	CAATCACGATTGTCAGGCAGTCGGCCAGCAGCCTGAAGTTGTCAGGATC
hbbe3:151-200	CTTTGACTTTTGGGTTAGCCATGATTGCCTCTGTGTTGTATAGGTTTCC
hbbe3:286-335	CTAACAGCCGGAAATTGCCTGGGTCGACTTGTAGTTTCTCTGAGTGAAG
hbbe2:95-143	CTCATAGTTGAGTTTGCTGAAGATGTCCTGGATGAAGGCACGTTCCTC
hbbe1.3:142-189	GCGAAGTACCGCTGGGTCCAGGGGTACACGATGAGACACCTTGCCAG
hbbe3:188-235	CTTTTCAAGTCCCTTGAGGACCACAACACCGTGCGCTTTGACTTTTG
hbbe1.2:126-171	CAGGGGTACACGATAAGACACCTTGCCAGAGCCTGAGGACCGATG
hbbe1.1:180-223	GATGGCAGCGGCATTGTAGAGGTTTCCAAACTTGGCGAAGTAC
hbbe1.2:336-379	CAAAAGCCTGAAGTTGTCGGGATCTACGTGGAGCTTCTCGGAG
hbbe2:304-346	CTCAGCTCGGCGTAGGTGTTCTTGATGTCATCCATGTTCTTC
hbbe3:465-507	TTTCATAATGCATAAAACAATGGTACAATCACTTCTTTCGGT
hbbe1.1:1-41	TTCAGACTAAGTGTCTTAAACAGAAGCTGAAGAGTGCTGT
hbbe1.1:317-357	TCTACGTGGAGCTTCTCGGAGTGCAGCACACTTAAATCAG
hbbe1.1:504-544	ACATTCTTTAGTGGAAACATTATAATCTCTCTCTGTCTGT
hbbe1.2:260-300	TTGTCCATGTTCTTTACAGCCAGCTCCAGACCCTTGAGCA
hbbe1.3:107-147	GCCAGAGCCTGAGGACCAATGACATCGTAGTCAGCCTTGG
hbbe2:238-278	GACGGTTCCGTGGGCTGCGACCTTTGGGTTGTTAATGATG

hbbe2:410-450	CTGTGAAAGCGGCGCCCATGGTGGAGGCAATCACGATTGT
hbbe3:318-358	GATCACCACGGTCAGGCAGTCCGCTAACAGCCGGAAATTG

References

Ding, Y.& Liu, F. (2022). Protocol for isolation and ATAC-seq library construction of zebrafish red blood cells. *STAR Protocols*, *3*, 101889. https://doi.org/https://doi.org/10.1016/j.xpro.2022.101889

Ellett, F., Pase, L., Hayman, J. W., Andrianopoulos, A., & Lieschke, G. J. (2011). mpeg1 promoter transgenes direct macrophage-lineage expression in zebrafish. *Blood*, *117*(4), e49-56. https://doi.org/10.1182/blood-2010-10-314120

Ganis, J. J., Hsia, N., Trompouki, E., Jong, J. L. O. d., DiBiase, A., Lambert, J. S., Jia, Z., Sabo, P. J., Weaver, M., Sandstrom, R., Stamatoyannopoulos, J. A., Zhou, Y., & Zon, L. I. (2012). Zebrafish globin switching occurs in two developmental stages and is controlled by the LCR. *Developmental Biology*, *366*, 186-194.

Howe, K., Clark, M. D., Torroja, C. F., Torrance, J., Berthelot, C., Muffato, M., Collins, J. E., Humphray, S., McLaren, K., Postlethwait, J. H., Nüsslein-Volhard, C., Hubbard, T. J. P., Roest, H., Crollius, Rogers, J., & Stemple, D. L. (2013). The zebrafish reference genome sequence and its relationship to the human genome. *Nature*, *496*(7446), 498–503. https://doi.org/10.1038/nature12111

Renshaw, S. A., Loynes, C. A., Trushell, D. M. I., Elworthy, S., Ingham, P. W., & Whyte, M. K. B. (2006). A transgenic zebrafish model of neutrophilic inflammation. *Blood*, *108*(13), 3976–3978. https://doi.org/https://doi.org/10.1182/blood-2006-05-024075

Rueb, K. F. & Stachura, D. L. (2021). Using Flow Cytometry to Detect and Quantitate Altered Blood Formation in the Developing Zebrafish. *JoVE Journal of Visualized Experiments*, *170*. https://doi.org/10.3791/61035

CHAPTER 4

CONCLUSIONS

Our research has shown that *zmynd11* regulates expression of proliferative and lineage specific genes in primitive red blood cells of zebrafish, but the mechanism behind target gene dysregulation is not known. Guo et. al. and Wen et. al. provided evidence that ZMYND11 promotes alternative splicing and stalls RNA polymerase II, but I believe a very important part of ZMYND11's mechanism of target gene regulation is in its interaction with PRC1.6. So far, no one has investigated if *ZMYND11* and PRC1.6 could possibly work together or antagonize each other to ensure proper lineage specification. I would like to offer two possible scenarios for how zmynd11 and PRC1.6 could interact to control maturation and cell fate.

In the first scenario, ZMYND11's ability to modulate alternative splicing and stalling RNA polymerase II at target genes could be a way to regulate actively transcribed genes and fine tune gene expression early in the development of specific lineages, then eventually, as the lineage is further specified, the early expressed genes must be shut down in order to continue maturing. As a result, ZMYND11 recruits PRC1.6 to shut down expression of those genes permanently. For example, genes promoting proliferation must be shut off at some point in lineage specification, so ZMYND11 could recruit PRC1.6 to turn off these genes, so that lineage specific genes can be upregulated. Alternatively, in the second scenario, PRC1.6 could be repressing lineage specific genes early in cell development and, as a result, maintaining expression of proliferative genes. In this scenario, ZMYND11 would interrupt PRC1.6's repression of lineage specific genes, which would in turn repress genes promoting proliferation.

From our RNA-seq data, we can see that members of PRC1.6, including MGA, L3MBTL2, PCGF6, are expressed in primitive zebrafish red blood cells, so it is certainly possible that PRC1.6 is involved in blood cell development. Additionally, mutations in several members of PRC1.6 have been implicated in leukemia, so they must have a role in some capacity either independently or as part of PRC1.6 to regulate blood cell development (Attieh et al., 2013; Paoli et al., 2013; Tanaskovic et al., 2022)

Furthermore, I wonder if ZMYND11's interaction with histone methylases and demethylases regulates PRC1.6's ability to associate with target genes. PRC1.6 members L3MBTL2 and HP1gamma are chromatin readers and bind to differential states of lysine methylation. L3MBTL2 recognizes mono- and demethylated lysines H3K4, H3K9, H3K27, and H4K20 and HP1gamma binds to di- and tri-methylated H3K9. Interestingly, ZMYND11 has been shown to interact with KDM3B, which removes mono- and di-methylation on H3K9, as well as NSD1 and KMT2A, which dimethylates H3K36 and mono- and di-methylate H3K4, respectively. ZMYND11 could activate or inhibit the activity of methylases and demethylases to control the histone code of target genes. This could in turn, recruit or interrupt binding of PRC1.6 to target genes. What's more, is that many histone methylases and demethylases, including the ones known to interact with ZMYND11, are mutated in leukemias, showing how important these specific histone modifications are for proper blood development (Guarnera et al., 2024; Kim et al., 2023; Yang et al., 2021; Yoo et al., 2024; Zehtabcheh et al., 2025).

Using the *zmynd11-/-;lcr:GFP* zebrafish created by our lab, a series of experiments using CUT N RUN or some other method to capture chromatin enriched for a specific target protein would help resolve these questions. First, CUT N RUN experiments to find *zmynd11* target genes in 48hpf primitive red blood cells would reveal which genes are directly regulated by *zmynd11*.

When combined with our RNA-seq data, we can see if target genes are up or down regulated in the absence of *zmynd11*. Additionally, CUT N RUN experiments using antibodies against PRC1.6 members to determine which genes are occupied by PRC1.6 in *zmynd11-/- ; lcr:GFP* red blood cells vs wild type *lcr:GFP* could help uncover the mechanism of *zmynd11* target gene regulation. For example, if less PRC1.6 is found localized at its normal genomic locations in *zmynd11-/-; lcr:GFP* red blood cells vs wild type *lcr:GFP*, we can assume that ZMYND11 is recruiting it to those genes. Additionally, overlapping genes occupied by *zmynd11* and one or more members of PRC1.6 could reveal target genes regulated by their interaction. Additionally, measuring ubiquitination of Histone H2A at lysine 119 (H2AK119ub1) of target genes could be used as a read out of PRC1.6 activity. If *zmynd11* is recruiting PRC1.6 to ubiquitinate H2AK119, then we would expect less H2AK119ub1 of target genes in *zmynd11-/-;lcr:GFP* red blood cells and more H2AK119ub1 if *zmynd11* inhibits PRC1.6 binding. Lastly, assessing the amount of methylation on lysine residues that are presumably needed for PRC1.6 targeting through L3MBTL2 and HP1gamma could reveal a histone code required for PRC1.6 targeting or inhibition. Furthermore, if the histone methylation patterns required to recruit PRC1.6 are disrupted in *zmynd11-/-: lcr:GFP* red blood cells, this could suggest that *zmynd11* is modulating activity of histone methylases and demethylases to influence binding of PRC1.6. The difficulty in performing these experiments in zebrafish is that most antibodies are raised against human proteins/epitopes that do not always cross-react with zebrafish proteins due to low sequence homology, but if suitable antibodies can be found, these experiments would be relatively simple.

Ultimately, I want to know what the "missing subpopulation" is that we only see in wild type *lcr:GFP* red blood cells, but not *zmynd11-/-;lcr:GFP*. Given the dysregulation of lineage specific genes, it is reasonable to assume that the subpopulation is either in a more mature or less

mature state than the majority of red blood cells in wild type *lcr:GFP*, and all the *zmynd11-/-; lcr:GFP* red blood cells have either gotten stuck in an immature state or accelerated their maturation, respectively. To help resolve this question, a couple different methods could be used to observe the morphology of developing red blood cells. Since zebrafish embryos are transparent, confocal images could be used to measure the size and shape of red blood cells *in vivo*. Alternatively, blood cells can be isolated from embryos, fixed to a slide, and differentially stained to observe morphological changes in red blood cells of *zmynd11-/-;lcr:GFP* compared to wild type *lcr:GFP*. Another relatively easy experiment would be to analyze the distribution of GFP intensity in red blood cells over time. Starting at about 30-36hpf through 72hpf-96hpf, wild type embryos can be deyolked to isolate blood cells, then analyzed by flow cytometry to see if there is a shift from high to low or low to high GFP intensity as red blood cells develop.

Given that *ZMYND11* loss of function is seen in several types of leukemia and patients with *ZMYND11* haploinsufficiency experience recurrent infections, both of which affect the definitive wave, it would be interesting to know if there is also a problem with the definitive wave of blood development. To address this question, blood could be drawn from adult *zmynd11-/-* zebrafish for blood smears to visualize the morphology of cells and obtain differential cell counts. A minimally invasive procedure can allow multiple blood draws from the same fish overtime without having to euthanize, so the effect of *zmynd11* deficiency on blood cells can be measured at several intervals over the life of the fish (Zang et al., 2013).

References

Attieh, Y., Geng, Q.-R., DiNardo, C. D., Zheng, H., Jia, Y., Fang, Z.-H., Gañán-Gómez, I., Yang, H., Wei, Y., Kantarjian, H., & Garcia-Manero, G. (2013). Low frequency of H3.3 mutations and upregulated DAXX expression in MDS. *Blood*, *121*(19), 4009-4011. https://doi.org/https://doi.org/10.1182/blood-2012-11-466714

Guarnera, L., D'Addona, M., Bravo-Perez, C., & Visconte, V. (2024). KMT2A Rearrangements in Leukemias: Molecular Aspects and Therapeutic Perspectives. *Int. J. Mol. Sci.*, *25*(9023). https://doi.org/https://doi.org/10.3390/ijms25169023

Kim, J.-Y., Kim, K.-B., Eom, G. H., Choe, N., Kee, H. J., Son, H.-J., Oh, S.-T., Kim, D.-W., Pak, J. H., Baek, H. J., Kook, H., Hahn, Y., Kook, H., Chakravarti, D., & Seo, S.-B. (2023). KDM3B Is the H3K9 Demethylase Involved in Transcriptional Activation of lmo2 in Leukemia. *Molecular and Cellular Biology*, *32*(14). https://doi.org/https://doi.org/10.1128/MCB.00133-12

Paoli, L. D., Cerri, M., Monti, S., Rasi, S., Spina, V., Bruscaggin, A., Greco, M., Ciardullo, C., Famà, R., Cresta, S., Maffei, R., Ladetto, M., Martini, M., Laurenti, L., Forconi, F., Marasca, R., Larocca, L. M., Bertoni, F., Gaidano, G., & Rossi, D. (2013). MGA, a suppressor of MYC, is recurrently inactivated in high risk chronic lymphocytic leukemia. *Leuk Lymphoma*, *54*(5), 1087-1090. https://doi.org/10.3109/10428194.2012.723706

Tanaskovic, N., Dalsass, M., Filipuzzi, M., Ceccotti, G., Verrecchia, A., Nicoli, P., Doni, M., Olivero, D., Pasini, D., Koseki, H., Sabo, A., Bisso, A., & Amati, B. (2022). Polycomb group ring finger protein 6 suppresses Myc-induced lymphomagenesis. *Life Science Alliance*, *5*(8), e202101344 https://doi.org/https://doi.org/10.26508/lsa.202101344

Yang, C., Wang, K., Liang, Q., Tian, T.-T., & Zhong, Z. (2021). Role of NSD1 as potential therapeutic target in tumor. *Pharmacological Research*, *172*.

Yoo, J., Kim, G. W., Jeon, Y. H., Lee, S. W., & Kwon, S. H. (2024). Epigenetic roles of KDM3B and KDM3C in tumorigenesis and their therapeutic implications. *Cell Death and Disease*, *15*(451). https://doi.org/https://doi.org/10.1038/s41419-024-06850-z

Zang, L., Shimada, Y., Nishimura, Y., Tanaka, T., & Nishimura, N. (2013). A Novel, Reliable Method for Repeated Blood Collection from Aquarium Fish. *Zebrafish*, *10*(00).

Zehtabcheh, S., Samarkhazan, H. S., Asadi, M., Zabihi, M., Parkhideh, S., & Mohammadi, M. H. (2025). Insights into KMT2A rearrangements in acute myeloid leukemia: from molecular characteristics to targeted therapies. *Biomarker Research*, *13*(17). https://doi.org/https://doi.org/10.1186/s40364-025-00786-y